

# Ricci Flow and Bio–Reaction–Diffusion Systems

Vladimir G. Ivancevic and Tijana T. Ivancevic

## Abstract

This paper proposes geometric Ricci–flow as a general model for reaction–diffusion systems and dissipative solitons in mathematical biology.

**Keywords:** Ricci flow, reaction–diffusion equations, mathematical biology, dissipative solitons and breathers

## Contents

<b>1</b>	<b>Introduction</b>	<b>2</b>
<b>2</b>	<b>Parabolic reaction–diffusion equations</b>	<b>6</b>
2.1	1–component systems . . . . .	8
2.1.1	Kolmogorov–Petrovsky–Piscounov equation . . . . .	8
2.1.2	Swift–Hohenberg Equation . . . . .	9
2.1.3	Neural field theory . . . . .	10
2.2	2–component systems . . . . .	10
2.2.1	Brusselator . . . . .	11
2.2.2	Gierer–Meinhardt activator–inhibitor system . . . . .	12
2.2.3	Fitzhugh–Nagumo activator–inhibitor system . . . . .	12
2.3	3–component systems . . . . .	14
2.3.1	Oregonator . . . . .	14
2.4	Multi–phase tumor growth . . . . .	15
2.5	Temporal dynamics of Hopfield’s neural networks . . . . .	16
2.5.1	Neurons as functions . . . . .	16
2.5.2	Activation dynamics . . . . .	18
2.5.3	Hopfield’s overlaps . . . . .	19
2.5.4	Overlap dynamics . . . . .	21
2.5.5	Hebbian learning dynamics . . . . .	21
2.5.6	Neural attractor dynamics . . . . .	24
2.5.7	Associative bidirectional competitive net . . . . .	25

<b>3</b>	<b>Dissipative evolution under the Ricci flow</b>	<b>26</b>
3.1	Geometrization conjecture . . . . .	26
3.2	Heat-type evolution of curvatures and volumes . . . . .	28
3.3	Dissipative solitons . . . . .	33
3.4	Ricci breathers and solitons . . . . .	34
3.5	Heat equation and Ricci entropy . . . . .	35
3.6	Thermodynamic analogy . . . . .	37
<b>4</b>	<b>Appendix: Riemann and Ricci curvatures on a smooth <math>n</math>-manifold</b>	<b>38</b>

# 1 Introduction

Reaction–diffusion systems are systems involving constituents locally transformed into each other by chemical reactions and transported in space by diffusion. They arise, quite naturally, in chemistry and chemical engineering but also serve as a reference for the study of a wide range of phenomena encountered beyond the strict realm of chemical science such as environmental and life sciences. Reaction–diffusion systems in a closed vessel and in the absence of external forces evolve eventually to the state of chemical equilibrium, whereby the constituents involved are distributed uniformly in space and each elementary reactive step is counteracted by its inverse. It has long been realized that the approach to equilibrium can be both in the form of a simple exponential decay, or more involved transient behaviors associated with damped oscillations or non-trivial space dependencies including wave–like patterns. While the former found immediately a series of important applications such as the experimental measurement of the rate constants of chemical reactions, the latter were originally regarded as curiosities. The development of *irreversible thermodynamics* in the 1950’s and onwards provided an explanation of the origin of these two kinds of behaviors by linking them to time evolutions starting close to and far from equilibrium, respectively. Experiment and modelling on laboratory scale reactive systems such as the Belousov–Zhabotinski reaction confirmed this view. Still as long as reaction–diffusion processes were carried out in a closed thermostated reactor there was no way to analyze systematically what was going on since, by virtue of the second law of thermodynamics, the system was bound to reach sooner or later the state of equilibrium [1].

The most familiar quantitative description of reaction–diffusion systems is based on the assumption of decoupling between two kinds of processes occurring on widely different scales: (i) the evolution of the macroscopic variables, such as the concentrations or mole fractions and the temperature  $T$ ; and (ii) the dynamics at the molecular level, which merely provides the values of a set of phenomenological parameters entering in the description such as the rate constants of reaction  $k_i$  and the mass or heat diffusivity coefficients  $D_i$ .

This approach, referred as the *mean field description*, takes the form of a set of balance partial differential equations (PDEs):

$$\partial_t x_i = v_i(\{x_j\}, k_i) + D_i \nabla^2 x_i, \quad (\partial_t x_i \equiv \frac{\partial x_i}{\partial t}), \quad (i = 1, \dots, n), \quad (1)$$

where the two terms in the right hand side stand, successively, for the effect of the chemical reactions and of transport. For simplicity, it is usually assumed that there is no bulk motion (which amounts to discarding the effects of external forces), that there are no cross effects in transport and that Fick's or Fourier's laws describe adequately mass and heat transport [1].

On the other hand, the *Ricci flow equation* (or, the *parabolic Einstein equation*), introduced by R. Hamilton in 1982 [36], is the nonlinear heat-like evolution equation<sup>1</sup>

$$\partial_t g_{ij} = -2R_{ij}, \quad (2)$$

for a time-dependent Riemannian metric  $g = g_{ij}(t)$  on a smooth real<sup>2</sup>  $n$ -manifold  $M$  with the Ricci curvature tensor  $R_{ij}$ .<sup>3</sup> This equation roughly says that we can deform any metric on a 2D surface or  $n$ D manifold by the negative of its curvature; after *normalization* (see Figure 1), the final state of such deformation will be a metric with constant curvature. The factor of 2 in (2) is more or less arbitrary, but the negative sign is essential to insure a kind of global *volume exponential decay*,<sup>4</sup> since the Ricci flow equation (2) is a kind of

---

<sup>1</sup>The current hot topic in geometric topology is the Ricci flow, a Riemannian evolution machinery that recently allowed G. Perelman to prove the celebrated *Poincaré Conjecture*, a century-old mathematics problem (and one of the seven Millennium Prize Problems of the Clay Mathematics Institute) – and win him the 2006 Fields Medal (which he declined in a public controversy) [27]. The Poincaré Conjecture can roughly be put as a question: Is a closed 3D manifold  $M$  topologically a sphere if every closed curve in  $M$  can be shrunk continuously to a point? In other words, Poincaré conjectured: A simply-connected compact 3D manifold is diffeomorphic to the 3D sphere  $S^3$  (see e.g., [28]).

<sup>2</sup>For the related Kähler Ricci flow on complex manifolds, see e.g., [29, 30]

<sup>3</sup>This particular PDE (2) was chosen by Hamilton for much the same reason that A. Einstein introduced the Ricci tensor into his gravitation field equation,

$$R_{ij} - \frac{1}{2}g_{ij}R = 8\pi T_{ij},$$

where  $T_{ij}$  is the energy-momentum tensor. Einstein needed a symmetric 2-index tensor which arises naturally from the metric tensor  $g_{ij}$  and its first and second partial derivatives. The Ricci tensor  $R_{ij}$  is essentially the only possibility. In gravitation theory and cosmology, the Ricci tensor has the volume-decreasing effect (i.e., convergence of neighboring geodesics, see [32]).

<sup>4</sup>This complex geometric process is globally similar to a generic exponential decay ODE:

$$\dot{x} = -\lambda f(x),$$

for a positive function  $f(x)$ . We can get some insight into its solution from the simple exponential decay ODE,

$$\dot{x} = -\lambda x \quad \text{with the solution} \quad x(t) = x_0 e^{-\lambda t},$$

nonlinear generalization of the standard linear heat equation

$$\partial_t u = \Delta u. \quad (3)$$

Like the heat equation (3), the Ricci flow equation (2) is well behaved in forward time and acts as a kind of smoothing operator (but is usually impossible to solve in backward time). If some parts of a solid object are hot and others are cold, then, under the heat equation, heat will flow from hot to cold, so that the object gradually attains a uniform temperature. To some extent the Ricci flow behaves similarly, so that the Ricci curvature ‘tries’ to become more uniform [37], thus resembling a monotonic *entropy growth*,<sup>5</sup>  $\partial_t S \geq 0$ , which is due to the positive definiteness of the metric  $g_{ij} \geq 0$ , and naturally implying the *arrow of time* [33, 30, 29].

In a suitable local coordinate system, the Ricci flow equation (2) has a nonlinear heat-type form, as follows. At any time  $t$ , we can choose local harmonic coordinates so that the coordinate functions are locally defined harmonic functions in the metric  $g(t)$ . Then the Ricci flow takes the form (see e.g., [38])

$$\partial_t g_{ij} = \Delta_M g_{ij} + Q_{ij}(g, \partial g), \quad (4)$$

where  $\Delta_M$  is the Laplace–Beltrami differential operator<sup>6</sup> and  $Q$  is a lower-order term quadratic in  $g$  and its first order partial derivatives. From the analysis of nonlinear heat PDEs, one obtains existence and uniqueness of forward-time solutions to the Ricci flow (4) on some time interval, starting at any smooth initial metric  $g_0 = g_{ij}(0)$ .

As a simple example of the Ricci flow equations (2)–(4), consider a round spherical boundary  $S^2$  of the 3D ball radius  $r$ . The metric tensor on  $S^2$  takes the form

$$g_{ij} = r^2 \hat{g}_{ij},$$

---

(where  $x = x(t)$  is the observed quantity with its initial value  $x_0$  and  $\lambda$  is a positive decay constant), as well as the corresponding  $n$ th order rate equation (where  $n > 1$  is an integer),

$$\dot{x} = -\lambda x^n \quad \text{with the solution} \quad \frac{1}{x^{n-1}} = \frac{1}{x_0^{n-1}} + (n-1)\lambda t.$$

<sup>5</sup>Note that two different kinds of entropy functional have been introduced into the theory of the Ricci flow, both motivated by concepts of entropy in thermodynamics, statistical mechanics and information theory. One is Hamilton’s entropy, the other is Perelman’s entropy. While in Hamilton’s entropy, the scalar curvature  $R$  of the metric  $g_{ij}$  is viewed as the leading quantity of the system and plays the role of a probability density, in Perelman’s entropy the leading quantity describing the system is the metric  $g_{ij}$  itself. Hamilton established the monotonicity of his entropy along the volume-normalized Ricci flow on the 2-sphere  $S^2$  [41]. Perelman established the monotonicity of his entropy along the Ricci flow in all dimensions [34].

<sup>6</sup>The Laplace–Beltrami differential operator on functions on an  $n$ -manifold  $M$  with respect to the metric  $g$ , is given by

$$\Delta_M = \frac{1}{\sqrt{\det(g)}} \frac{\partial}{\partial x^i} \left( \sqrt{\det(g)} g^{ij} \frac{\partial}{\partial x^j} \right). \quad (5)$$

where  $\hat{g}_{ij}$  is the metric for a unit sphere, while the Ricci tensor

$$R_{ij} = (n - 1)\hat{g}_{ij}$$

is independent of  $r$ . The Ricci flow equation on  $S^2$  reduces to

$$\dot{r}^2 = -2(n - 1),$$

with solution

$$r^2(t) = r^2(0) - 2(n - 1)t.$$

Thus the boundary sphere  $S^2$  collapses to a point in finite time (see [37]).

More generally, the following geometrization conjecture holds for any 3-manifold  $M$ : Suppose that we start with a compact initial 3-manifold  $M_0$  whose Ricci tensor  $R_{ij}$  is everywhere positive definite. Then, as  $M_0$  shrinks to a point under the Ricci flow (2), it becomes rounder and rounder. If we rescale the metric  $g_{ij}$  on  $M_0$  so that the volume of  $M_0$  remains constant, then  $M_0$  converges towards another compact 3-manifold  $M_1$  of constant positive curvature (see [36]).

In case of even more general 3-manifolds (outside the class of positive Ricci curvature metrics), the situation is much more complicated, as various singularities may arise. One way in which singularities may arise during the Ricci flow is that a spherical boundary  $S^2 = \partial M$  of an 3-manifold  $M$  may collapse to a point in finite time. Such collapses can be eliminated by performing a kind of “geometric surgery” on the 3-manifold  $M$ , that is a sophisticated sequence of cutting and pasting without accumulation of time errors<sup>7</sup> (see [35]). After a finite number of such surgeries, each component either: (i) converges towards a 3-manifold of constant positive Ricci curvature which shrinks to a point in finite time, or possibly (ii) converges towards an  $S^2 \times S^1$  which shrinks to a circle  $S^1$  in finite time, or (iii) admits a “thin-thick” decomposition of [43]. Therefore, one can choose the surgery parameters so that there is a well defined Ricci-flow-with surgery, that exists for all time [35].

In this paper we use the evolving geometric machinery of the volume-decaying and entropy-growing Ricci flow  $g(t)$ , given by equations (2)–(4), for modelling general biological dissipative solitons.

---

<sup>7</sup>Hamilton’s idea was to perform surgery to cut off the singularities and continue his flow after the surgery. If the flow develops singularities again, one repeats the process of performing surgery and continuing the flow. If one can prove there are only a finite number of surgeries in any finite time interval, and if the long-time behavior of solutions of the Ricci flow (2) with surgery is well understood, then one would be able to recognize the topological structure of the initial manifold. Thus Hamilton’s program, when carried out successfully, would lead to a proof of the Poincaré conjecture and Thurston’s geometrization conjecture [28].

## 2 Parabolic reaction–diffusion equations

Parabolic reaction–diffusion systems of the type (1) are abundant in mathematical biology. They are mathematical models that describe how the concentration of one or more substances distributed in space changes under the influence of two processes: local chemical reactions in which the substances are converted into each other, and diffusion which causes the substances to spread out in space. More formally, they are expressed as semi-linear parabolic PDEs (see e.g., [7]. The evolution of the state vector  $\mathbf{u}(\mathbf{x}, t)$  describing the concentration of the different reagents is determined by anisotropic<sup>8</sup> diffusion as well as local reactions:

$$\partial_t \mathbf{u} = \mathbf{D} \Delta \mathbf{u} + \mathbf{R}(\mathbf{u}), \quad (6)$$

where each component of the state vector  $\mathbf{u}(\mathbf{x}, t)$  represents the concentration of one substance,  $\mathbf{D}$  is a symmetric positive-definite matrix of diffusion coefficients (which are proportional to the velocity of the diffusing particles) and  $\mathbf{R}(\mathbf{u})$  accounts for all local reactions. The solutions of reaction–diffusion equations display a wide range of behaviors, including the formation of travelling waves<sup>9</sup> and wave-like phenomena as well as other self-organized patterns<sup>10</sup> like stripes, hexagons or more intricate structure like dissipative solitons (DSs).

The driving force for the diffusion (in case of ideal mixtures) is the concentration gradient  $-\nabla u$ , or (in general) the gradient of the chemical potential  $-\nabla u_i$  of each species  $u_i$ , giving the *diffusion flux* by the Fick’s first law,

$$J = -\mathbf{D} \nabla \mathbf{u}. \quad (7)$$

---

<sup>8</sup>Anisotropy is the property of being directionally dependent, as opposed to isotropy, which means homogeneity in all directions. For example, magnetic anisotropy may occur in a plasma, so that its magnetic field is oriented in a preferred direction. Plasmas may also show ‘filamentation’ (such as that seen in lightning or a plasma globe) that is directional. An anisotropic liquid (e.g., liquid crystal) is one which has the fluidity of a normal liquid, but has an average structural order relative to each other along the molecular axis, unlike water or chloroform, which contain no structural ordering of the molecules.

<sup>9</sup>Travelling wave is a disturbance  $u(x, t)$  of a medium that varies both with time  $t$  and distance  $x$  as

$$u(x, t) = A(x, t) \sin(kx - \omega t + \phi),$$

where  $A(x, t)$  is the amplitude envelope of the wave,  $k$  is the wave number and  $\phi$  is the phase. Its phase velocity  $v_p$  is given by

$$v_p = \omega/k = \lambda f,$$

where  $\lambda$  is the wavelength.

<sup>10</sup>Self-organization is a process of attraction and repulsion in which the internal organization of a system, normally an open system, increases in complexity without being guided or managed by an outside source. Self-organizing systems usually display emergent properties (that is, the way complex systems and patterns arise out of a multiplicity of relatively simple interactions). Self-organization typically relies on four basic ingredients: (i) positive (amplifying) feedback, (ii) negative (homeostatic) feedback, (iii) balance of exploitation and exploration, and (iv) multiple interactions.

Assuming the diffusion coefficients  $\mathbf{D}$  to be a constant, the Second Fick's law gives the parabolic *heat equation*,

$$\partial_t \mathbf{u} = \mathbf{D} \Delta \mathbf{u}, \quad (8)$$

while, in case of variable diffusion coefficients  $\mathbf{D}$ ,<sup>11</sup> we get (slightly) more general parabolic *diffusion equation*,

$$\partial_t \mathbf{u} = \nabla \cdot (\mathbf{D} \nabla \mathbf{u}). \quad (9)$$

The diffusion coefficient  $D = D(T)$  at different temperatures  $T$  can be approximated by the *Arrhenius exponential-decay relation*,

$$D(t) = D_0 \cdot e^{-\frac{E_A}{rT}},$$

where  $D_0$  is the maximum possible diffusion coefficient (at infinite temperature  $T$ ),  $E_A$  is the activation energy for diffusion (i.e., the energy that must be overcome in order for a chemical reaction to occur) and  $r$  is the gas constant.

Using the Fick's first law (7), the diffusion equation (9) can be derived in a straightforward way from the continuity equation, which states that a change in density in any part of the system is due to inflow and outflow of material into and out of that part of the system (effectively, no material is created or destroyed),

$$\partial_t u + \nabla \cdot \mathbf{j} = 0,$$

where  $\mathbf{j}$  is the flux of the diffusing material.

The most important special case of (74) is at a steady state, when the concentrations  $\mathbf{u}$  do not change in time, giving the Laplace's equation,

$$\Delta \mathbf{u} = 0, \quad \text{or} \quad \Delta u_i = 0, \quad (10)$$

for harmonic functions  $\mathbf{u} = \{u_i\}$ .

The stochastic version of the deterministic heat equation (74), connected with the study of Brownian motion,<sup>12</sup> is the *Fokker-Planck equation*,

$$\partial_t f = -\partial_{x^i} [D_i^1(x^i) f] + \partial_{x^i x^j} [D_{ij}^2(x^i) f], \quad (11)$$

---

<sup>11</sup>The diffusion coefficient  $D = D(T)$  at different temperatures  $T$  can be approximated by the *Arrhenius exponential-decay relation*,

$$D(t) = D_0 \cdot e^{-\frac{E_A}{R \cdot T}},$$

where  $D_0$  is the maximum possible diffusion coefficient (at infinite temperature  $T$ ),  $E_A$  is the activation energy for diffusion and  $R$  is the gas constant.

<sup>12</sup>Brownian motion is the random movement of particles suspended in a liquid or gas or the mathematical model used to describe such random movements, often called a particle theory. The infinitesimal generator (and hence characteristic operator) of a Brownian motion on  $\mathbb{R}^n$  is  $\frac{1}{2}\Delta$ , where  $\Delta$  is the Laplacian on  $\mathbb{R}^n$ . More generally, a Brownian motion on an  $n$ -manifold  $M$  is given by one-half of the Laplace-Beltrami operator  $\Delta_M$  (5).

( $\partial_{x^i} = \frac{\partial}{\partial x_i}$ ,  $\partial_{x^i x^j} = \frac{\partial^2}{\partial x_i \partial x_j}$ ), where  $D_i^1$  is the drift vector and  $D_{ij}^2$  the diffusion tensor (which results from the presence of the stochastic force). The Fokker–Planck equation (11) is used for computing the probability densities of stochastic differential equations.<sup>13</sup>

Also, notice that the real-valued heat equation (74) is formally similar to the complex-valued *Schrödinger equation*,

$$\partial_t \psi = \frac{i\hbar}{2m} \Delta \psi, \quad (12)$$

where  $\psi = \psi(\mathbf{x}, t)$  is the wave-function of the particle,  $i = \sqrt{-1}$ , and  $\hbar$  is Planck’s constant divided by  $2\pi$ .

## 2.1 1-component systems

### 2.1.1 Kolmogorov–Petrovsky–Piscounov equation

The simplest reaction–diffusion equation concerning the concentration  $u$  of a single substance in one spatial dimension,

$$\partial_t u = D \partial_x^2 u + R(u), \quad (13)$$

is also referred to as the Kolmogorov–Petrovsky–Piscounov (KPP) equation. If the reaction term vanishes, then the equation represents a pure diffusion process described by the *heat equation*. In particular, the choice

$$R(u) = u(1 - u)$$

yields *Fisher’s equation* that was originally used to describe the spreading of biological populations.

The one-component KPP equation (13) can also be written in the variational (gradient) form

$$\partial_t u = -\frac{\delta F}{\delta u}, \quad (14)$$

---

<sup>13</sup>Consider the Itô stochastic differential equation,

$$d\mathbf{X}_t = \boldsymbol{\mu}(\mathbf{X}_t, t) dt + \boldsymbol{\sigma}(\mathbf{X}_t, t) d\mathbf{W}_t,$$

where  $\mathbf{X}_t \in \mathbb{R}^n$  is the state of an  $n$ D stochastic system at time  $t$  and  $\mathbf{W}_t \in \mathbb{R}^m$  is the standard  $m$ D Wiener process. If the initial distribution is  $\mathbf{X}_0 \sim f(\mathbf{x}, 0)$ , then the probability density of the state is given by the Fokker–Planck equation (11) with the drift and diffusion terms,

$$D_i^1(\mathbf{x}, t) = \mu_i(\mathbf{x}, t) \quad \text{and} \quad D_{ij}^2(\mathbf{x}, t) = \frac{1}{2} \sum_k \sigma_{ik}(\mathbf{x}, t) \sigma_{kj}^\top(\mathbf{x}, t).$$



and therefore describes a permanent decrease (a kind of exponential decay) of the system's *free energy* functional

$$F = \int_{-\infty}^{\infty} \left[ \frac{D}{2} (\partial_x u)^2 + V(u) \right] dx,$$

where  $V(u)$  is the potential such that

$$R(u) = -\frac{dV(u)}{du}. \quad (15)$$

### 2.1.2 Swift–Hohenberg Equation

The Swift–Hohenberg (SH) equation, noted for its pattern-forming behavior, is given by

$$\partial_t u = R(u) - (1 + \Delta)u, \quad (16)$$

representing a variational (gradient) equation (14) with the free energy functional

$$F = \int_{\Omega} \left[ V(u) + \frac{1}{2} ((1 + \Delta)u)^2 \right] dxdy,$$

where  $R(u)$  is given by (15), while  $\Omega$  is a 2D region in which pattern formation occurs.

The time derivative of the free energy  $F$  is given by

$$\partial_t F = \int_{\Omega} \left[ \frac{dV(u)}{du} + (1 + \Delta)u \right] \partial_t u \, dxdy,$$

and, since the expression in square brackets is equal to the negative right-hand side of (16), we have

$$\dot{F} = - \int_{\Omega} (\partial_t u)^2 \, dxdy \leq 0.$$

Therefore, the free energy  $F$  is the *Lyapunov functional* that may only decrease as it evolves along its trajectory in some phase space. If  $F$  has no minima, then when the horizontal scale of the liquid container is large compared to the instability wavelength, a propagating front will be observed (e.g., in chemically reacting flames). In this case,  $F$  will decrease continuously until the front approaches the boundary of the medium. An alternative possibility is realized when  $F$  has one or several minima, each corresponding to a local equilibrium state in time. In this case the so-called multi-stability is possible. Therefore, the limit behavior of gradient systems of the form of (15) is characterized by either a steady attractor or propagating fronts [16].

### 2.1.3 Neural field theory

The dynamical system from which the temporal evolution of neural activation fields is generated is constrained by the postulate that localized peaks of activation are stable objects, or, in mathematical terms, *fixed point attractors*. Such a field dynamics has the generic form [20]

$$\tau \partial_t u = -u + \text{resting level} + \text{input} + \text{interaction}, \quad (17)$$

where  $u = u(x, t)$  is the activation field defined over the metric dimension  $x$  and time  $t$ . The first three terms define an input driven regime, in which attractor solutions have the form

$$u(x, t) = \text{resting level} + \text{input}.$$

The *rate of relaxation* is determined by the time scale parameter  $\tau$ . The interaction stabilizes localized peaks of activation against decay by local excitatory interaction and against diffusion by global inhibitory interaction. In Amari's formulation [21] the conceptual model (17) is specified as a *continuous model for neural activity in cortical structures*,

$$\tau \partial_t u(x, t) = -u(x, t) + h + S(x, t) + \int dx' w(x - x') \sigma(u(x', t)), \quad (18)$$

where  $h < 0$  is a constant resting level,  $S(x, t)$  is spatially and temporally variable input function,  $w(x)$  is an interaction kernel and  $\sigma(u)$  is a sigmoidal nonlinear threshold function. The interaction term collects input from all those field sites  $x'$  at which activation is sufficiently large. The interaction kernel determines if inputs from those sites are positive, driving up activation (excitatory), or negative, driving down activation (inhibitory). Excitatory input from nearby location and inhibitory input from all field locations generically stabilizes localized peaks of activation. For this class of dynamics, detailed analytical results provide a framework for the inverse dynamics task facing the modeler, determining a dynamical system that has the appropriate attractor solutions [19].

## 2.2 2-component systems

Two-component systems allow for a much larger range of possible phenomena than their one-component counterparts. An important idea that was first proposed by A. Turing is that a state that is stable in the local system should become unstable in the presence of diffusion [5]. This idea seems counter-intuitive at first glance as diffusion is commonly associated with a stabilizing effect. However, the linear stability analysis shows that when linearizing the general two-component system

$$\begin{pmatrix} \partial_t u \\ \partial_t v \end{pmatrix} = \begin{pmatrix} D_u & 0 \\ 0 & D_v \end{pmatrix} \begin{pmatrix} \partial_{xx} u \\ \partial_{xx} v \end{pmatrix} + \begin{pmatrix} F(u, v) \\ G(u, v) \end{pmatrix}$$

and perturbing the system against plane waves

$$\tilde{\mathbf{u}}_{\mathbf{k}}(\mathbf{x}, t) = \begin{pmatrix} \tilde{u}(t) \\ \tilde{v}(t) \end{pmatrix} e^{i\mathbf{k} \cdot \mathbf{x}}$$

close to a stationary homogeneous solution one finds [52]

$$\begin{pmatrix} \partial_t \tilde{u}_{\mathbf{k}}(t) \\ \partial_t \tilde{v}_{\mathbf{k}}(t) \end{pmatrix} = -k^2 \begin{pmatrix} D_u \tilde{u}_{\mathbf{k}}(t) \\ D_v \tilde{v}_{\mathbf{k}}(t) \end{pmatrix} + \mathbf{R}' \begin{pmatrix} \tilde{u}_{\mathbf{k}}(t) \\ \tilde{v}_{\mathbf{k}}(t) \end{pmatrix}.$$

Turing’s idea can only be realized in four equivalence classes of systems characterized by the signs of the Jacobian  $\mathbf{R}'$  of the reaction function. In particular, if a finite wave vector  $\mathbf{k}$  is supposed to be the most unstable one, the Jacobian must have the signs

$$\begin{pmatrix} + & - \\ + & - \end{pmatrix}, \quad \begin{pmatrix} + & + \\ - & - \end{pmatrix}, \quad \begin{pmatrix} - & + \\ - & + \end{pmatrix}, \quad \begin{pmatrix} - & - \\ + & + \end{pmatrix}.$$

This class of systems is named activator–inhibitor system after its first representative: close to the ground state, one component stimulates the production of both components while the other one inhibits their growth. Its most prominent representative is the FitzHugh–Nagumo equation (20).

### 2.2.1 Brusselator

Classical model of an autocatalytic chemical reaction is Prigogine’s Brusselator (see e.g., [2])

$$\begin{aligned} \partial_t u &= D_u^2 \Delta u + \alpha + u^2 v - (1 + \beta)u, \\ \partial_t v &= D_v^2 \Delta v - u^2 v + \beta u, \end{aligned} \tag{19}$$

which describe the spatio–temporal evolution of the intermediate components  $u$  and  $v$ , with diffusion coefficients  $D_u$  and  $D_v$ , while reactions



describe the concentration of the original substances  $\alpha$  and  $\beta$ , for which the final products  $c$  and  $d$  are constant when all four reaction rates  $r_i$  equal unity.

A discretized (temporal only) version of the Brusselator PDE–model (19) reads

$$\begin{aligned} \dot{u} &= \alpha + u^2 v - (1 + \beta)u, \\ \dot{v} &= \beta u - u^2 v. \end{aligned}$$

The Brusselator displays oscillatory behavior in the species  $u$  and  $v$  when reverse reactions are neglected and the concentrations of  $\alpha$  and  $\beta$  are kept constant.

### 2.2.2 Gierer–Meinhardt activator–inhibitor system

Spontaneous pattern formation in initially almost homogeneous systems is common in both organic and inorganic systems. The Gierer–Meinhardt model [10] is a reaction–diffusion system of the activator–inhibitor type that appears to account for many important types of pattern formation and morphogenesis observed in biology, chemistry and physics. The model describes the concentration of a short–range autocatalytic substance, the activator, that regulates the production of its long–range antagonist, the inhibitor. It is given as a 2–component nonlinear PDE system,

$$\begin{aligned}\partial_t a &= -\mu_a a + \rho a^2/h + D_a \partial_{x^2} a + \rho_a, \\ \partial_t h &= -\mu_h h + \rho a^2 + D_h \partial_{x^2} h + \rho_h,\end{aligned}$$

where  $a$  is a short–range autocatalytic substance, i.e., *activator*, and  $h$  is its long–range antagonist, i.e., *inhibitor*.  $\partial_t a$  and  $\partial_t h$  describe respectively the changes of activator and inhibitor concentrations per second,  $\mu_a$  and  $\mu_h$  are the corresponding decay rates, while  $D_a$  and  $D_h$  are the corresponding diffusion coefficients.  $\rho$  is a positive constant.  $\rho_a$  is a small activator–independent production rate of the activator and is required to initiate the activator autocatalysis at very low activator concentration, e.g., in the case of regeneration. A low baseline production of the inhibitor,  $\rho_h$ , leads to a stable non–patterned steady state; the system can be asleep until an external trigger occurs by an elevation of the activator concentration above a threshold.

Common in the pattern–forming systems is that a deviation from homogeneity has a strong positive feedback on its further increase. For example, erosion proceeds faster at an initial small depression since more water collects there, deepening further the depression. In the case of sand dunes, a small elevation resembles a wind shelter behind which more sand becomes deposited. However, self–enhancement is not sufficient. On its own, it would lead to an unlimited increase and spreading. Pattern formation requires in addition a longer ranging confinement of the locally self–enhancing process. This limitation can either result from a long–ranging inhibitory signalling that spreads rapidly from such a region. Alternatively the antagonistic effect can result from a depletion of material required for the self–enhancement that is obtained from the surrounding region [11].

### 2.2.3 Fitzhugh–Nagumo activator–inhibitor system

Another frequently encountered example of reaction–diffusion systems is the two–component Fitzhugh–Nagumo–type activator–inhibitor system [17, 18],

$$\begin{aligned}\tau_u \partial_t u &= D_u^2 \Delta u + f(u) - \sigma v, \\ \tau_v \partial_t v &= D_v^2 \Delta v + u - v,\end{aligned}\tag{20}$$

with  $f(u) = \lambda u - u^3 - \kappa$ , which describes how an action potential travels through a nerve,  $D_u$  and  $D_v$  are diffusion coefficients,  $\tau_u$  and  $\tau_v$  are time characteristics, while  $\kappa, \sigma$  and  $\lambda$  are positive constants. In matrix form, system (20) reads

$$\begin{pmatrix} \tau_u \partial_t u \\ \tau_v \partial_t v \end{pmatrix} = \begin{pmatrix} D_u^2 & 0 \\ 0 & D_v^2 \end{pmatrix} \begin{pmatrix} \Delta u \\ \Delta v \end{pmatrix} + \begin{pmatrix} \lambda u - u^3 - \kappa - \sigma v \\ u - v \end{pmatrix}.$$

When an activator–inhibitor system undergoes a change of parameters, one may pass from conditions under which a homogeneous ground state is stable to conditions under which it is linearly unstable. The corresponding bifurcation may be either a *Hopf bifurcation* to a globally oscillating homogeneous state with a dominant wave number  $k = 0$  or a *Turing bifurcation* to a globally patterned state with a dominant finite wave number. The latter in two spatial dimensions typically leads to stripe or hexagonal patterns.

In particular, for the Fitzhugh–Nagumo system (20), the neutral stability curves marking the boundary of the linearly stable region for the Turing and Hopf bifurcation are given by

$$\begin{aligned} q_n^H(k) : \quad \frac{1}{\tau} + (d_u^2 + \frac{1}{\tau} d_v^2) k^2 &= f'(u_h), \\ q_n^T(k) : \quad \frac{\kappa_3}{1 + d_v^2 k^2} + d_u^2 k^2 &= f'(u_h). \end{aligned}$$

If the bifurcation is subcritical, often localized structures (i.e., dissipative solitons) can be observed in the hysteretic region where the pattern coexists with the ground state. Other frequently encountered structures comprise pulse trains, spiral waves and target patterns.

The reduced (temporal) 2D non–dimensional Fitzhugh–Nagum equations read:

$$\dot{v} = v(a - v)(v - 1) - w + I_a, \quad (21)$$

$$\dot{w} = bv - \gamma w, \quad (22)$$

where  $0 < a < 1$  is essentially the threshold value,  $b$  and  $\gamma$  are positive constants and  $I_a$  is the applied current. The drift field for this model is given by

$$u_1(v, w) = v(a - v)(v - 1) - w, \quad u_2(v, w) = bv - \gamma w.$$

As can be seen from (22) the null cline of the deterministic dynamics of this equations is the line  $v = \frac{\gamma}{b}w$ . By substitution on the r.h.s of equation (21) we find the following equation for steady states

$$v(a - v)(v - 1) - \frac{b}{\gamma}v = 0.$$

When this system is in a noisy environment, in the limit of weak noise, we can approximate the dynamics of the fluctuations by the 1D *Langevin equation*

$$\dot{v} = v(a - v)(v - 1) - \frac{b}{\gamma}v + \xi(t),$$

that is, the fluctuations run along the line  $v = \frac{\gamma}{b}w$ .

In particular, parameters in the *FitzHugh–Nagumo neuron* model [19]

$$\dot{v} = a + bv + cv^2 + dv^3 - u, \quad \dot{u} = \varepsilon(ev - u),$$

can be tuned so that the model describes spiking dynamics of many resonator neurons. Since one needs to simulate the shape of each spike, the time step in the model must be relatively small, e.g.,  $\tau = 0.25 \text{ ms}$ . Since the model is a  $2D$  system of ODEs, without a reset, it cannot exhibit autonomous chaotic dynamics or bursting. Adding noise to this, or some other  $2D$  models, allows for stochastic bursting.

## 2.3 3–component systems

### 2.3.1 Oregonator

The Oregonator model is based on the so-called FKN–mechanism [12], which provided the first successful explanation of the chemical oscillations that occur in the BZ reaction. It is composed of five coupled elementary chemical stoichiometries. During the last two decades, the Oregonator model has been modified in many ways by inclusion of additional chemical reaction steps or by changing the rate constants. If we denote the concentration of the species  $S$  by  $[S]$ , then we define:  $A = [\text{BrO}_3^-]$ ,  $H = [\text{H}^+]$ ,  $X = [\text{HBrO}_2]$ ,  $Y = [\text{Br}^-]$ ,  $Z = [\text{Ce}^{4+}]$ . The original Oregonator model was described by the following three coupled nonlinear PDEs,

$$\begin{aligned} \partial_t X &= k_1 A H^2 Y - k_2 H X Y - 2k_3 X^2 + k_4 A H X + D_X \nabla_{\mathbf{r}}^2 X, \\ \partial_t Y &= -k_1 A H^2 Y - k_2 H X Y + k_5 f Z + D_Y \nabla_{\mathbf{r}}^2 Y, \\ \partial_t Z &= 2k_4 A H X - k_5 Z + D_Z \nabla_{\mathbf{r}}^2 Z, \end{aligned} \tag{23}$$

where  $f$  is a stoichiometric factor [14],  $k_i$  ( $i = 1, \dots, 5$ ) are rate constants, while  $D_X$ ,  $D_Y$ , and  $D_Z$  are the diffusion constants of the species  $\text{HBrO}_2$ ,  $\text{Br}^-$ , and  $\text{Ce}^{4+}$  respectively (for dilute solutions, the diffusion matrix is diagonal). For a thorough discussion of the chemistry on which the Oregonator is based, the reader is referred to [13].

The Oregonator temporal mass–action dynamics is a well–stirred, homogeneous system of ODEs given by

$$\begin{aligned} \dot{X} &= k_1 A Y - k_2 X Y + k_3 A X - 2k_4 X^2, \\ \dot{Y} &= -k_1 A Y - k_2 X Y + 1/2 k_c f B Z, \\ \dot{Z} &= 2k_3 A X - k_c B Z, \end{aligned}$$

which are typically scaled as [13]

$$\begin{aligned}\epsilon(dx/d\tau) &= qy - xy + x(1 - x), \\ \epsilon'(dy/d\tau) &= -qy - xy + fz, \\ dz/d\tau &= x - z.\end{aligned}$$

The basic chemistry of the BZ-oscillations involves jumps between high and low HBrO<sub>2</sub> ( $X$ ) states, which is reflected in the relaxation oscillator nature of the Oregonator. This fundamental bistability may be stabilized in a flow reactor (CSTR) with reactants and Br<sup>-</sup> in the feed stream. Hysteresis between the two states is observed both experimentally and in the Oregonator. Quasiperiodicity and chaos also are observed in CSTR and can be modeled by the Oregonator [15].

## 2.4 Multi-phase tumor growth

A general model of multi-phase tumor growth is given in [9] by the parabolic reaction-diffusion PDE,

$$\partial_t \Phi_i = \nabla \cdot (D_i \Phi_i) - \nabla \cdot (\mathbf{v}_i \Phi_i) + \lambda_i(\Phi_i, C_i) - \mu_i(\Phi_i, C_i) \quad (24)$$

( $\partial_t \equiv \partial/\partial t$ ), where for phase  $i$ ,  $\Phi_i$  is the volume fraction ( $\sum_i \Phi_i = 1$ ),  $D_i$  is the random motility or diffusion,  $\lambda_i(\Phi_i, C_i)$  is the chemical and phase dependent production, and  $\mu_i(\Phi_i, C_i)$  is the chemical and phase dependent degradation/death, and  $\mathbf{v}_i$  is the cell velocity defined by the constitutive equation

$$\mathbf{v}_i = -\mu \nabla p, \quad (25)$$

where  $\mu$  is a positive constant describing the viscous-like properties of tumor cells and  $p$  is the spheroid internal pressure.

In particular, the multi-phase equation (24) splits into two heat-like mass-conservation PDEs [9],

$$\partial_t \Phi^C = S^C - \nabla \cdot (\mathbf{v}^C \Phi^C), \quad \partial_t \Phi^F = S^F - \nabla \cdot (\mathbf{v}^F \Phi^F), \quad (26)$$

where  $\Phi^C$  and  $\Phi^F$  are the tissue cell/matrix and fluid volume fractions, respectively,  $\mathbf{v}^C$  and  $\mathbf{v}^F$  are the cell/matrix and the fluid velocities (both defined by their constitutive equations of the form of (25)),  $S^C$  is the rate of production of solid phase tumor tissue and  $S^F$  is the creation/degradation of the fluid phase. Conservation of matter in the tissue,  $\Phi^C + \Phi^F = 1$ , implies that  $\nabla \cdot (\mathbf{v}^C \Phi^C + \mathbf{v}^F \Phi^F) = \Phi^C + \Phi^F$ . The assumption that the tumor may be described by two phases only implies that the new cell/matrix phase is formed from the fluid phase and vice versa, so that  $S^C + S^F = 0$ . The detailed biochemistry of tumor growth can be coupled into the model above through the growth term  $S^C$ , with equations added for nutrient diffusion, see [9] and references therein.

The multi-phase tumor growth model (24) has been derived from the classical transport/mass conservation equations for different chemical species [9],

$$\partial_t u_i = P_i - \nabla \cdot \mathbf{N}_i. \quad (27)$$

Here  $C_i$  are the concentrations of the chemical species, subindex  $a$  for oxygen,  $b$  for glucose,  $c$  for lactate ion,  $d$  for carbon dioxide,  $e$  for bicarbonate ion,  $f$  for chloride ion, and  $g$  for hydrogen ion concentration;  $P_i$  is the net rate of consumption/production of the chemical species both by tumor cells and due to the chemical reactions with other species; and  $\mathbf{N}_i$  is the flux of each of the chemical species inside the tumor spheroid, given (in the simplest case of uncharged molecules of glucose,  $O_2$  and  $CO_2$ ) by Fick's law,

$$\mathbf{N}_i = -D_i \nabla u_i,$$

where  $D_i$  are (positive) constant diffusion coefficients. In case of charged molecules of ionic species, the flux  $\mathbf{N}_i$  contains also the (negative) gradient of the volume fractions  $\Phi_i$ .

A popular example of reaction-diffusion systems is Swift-Hohenberg PDE (Swift-Hohenberg equation),

$$\partial_t u = ru - (1 + \nabla^2)^2 u + N(u),$$

where  $u = u(x, t)$  or  $u = u(x, y, t)$  is a scalar function defined on the line or the plane,  $r$  is a real bifurcation parameter, and  $N(u)$  is some smooth nonlinearity.

## 2.5 Temporal dynamics of Hopfield's neural networks

### 2.5.1 Neurons as functions

It is a common view in computational intelligence that neurons behave as functions (see [57, 24, 25]): they transduce an unbounded input *activation*  $x(t)$  into output *signal*  $S(x(t))$ . Usually a sigmoidal (S-shaped, bounded, monotone-nondecreasing:  $S' \geq 0$ ) function describes the transduction, as well as the input-output behavior of many operational amplifiers. For example, the *logistic signal* (or, the *maximum-entropy*) function

$$S(x) = \frac{1}{1 + e^{-cx}}$$

is sigmoidal and strictly increases for positive scaling constant  $c > 0$ . Strict monotonicity implies that the *activation derivative* of  $S$  is positive:

$$S' = \frac{dS}{dx} = cS(1 - S) > 0.$$

Another frequent bipolar signal function is the *hyperbolic-tangent*,

$$S(x) = \tanh(cx) = \frac{e^{cx} - e^{-cx}}{e^{cx} + e^{-cx}},$$



with activation derivative

$$S' = c(1 - S^2) > 0.$$

Also, the *Gaussian*, or bell-shaped, signal function of the form  $S(x) = e^{-cx^2}$ , for  $c > 0$ , represents an important exception to signal monotonicity. Its activation derivative  $S' = -2cxe^{-cx^2}$  has the sign opposite the sign of the activation  $x$ .

The *signal velocity*  $\dot{S} \equiv dS/dt$  is the *signal time derivative*, related to the activation derivative by

$$\dot{S} = S'\dot{x},$$

so it depends explicitly on *activation velocity*. This is used in unsupervised learning laws that adapt with *locally available information*.

The signal  $S(x)$  induced by the activation  $x$  represents the neuron's firing frequency of action potentials, or pulses, in a sampling interval. The firing frequency equals the average number of pulses emitted in a sampling interval.

*Short-term memory* is modelled by *activation dynamics*, and *long-term memory* is modelled by *learning dynamics*. The overall neural network behaves as an *adaptive filter* (see [58]).

Continuous ANNs are *temporal dynamical systems* with two coupled dynamics: activation and learning. First, a general system of coupled ODEs for the output of the  $i$ th *processing element* (PE)  $x^i$ , called the *activation dynamics*, can be written as

$$\dot{x}^i = g_i(x^i, \text{net}_i), \quad (28)$$

with the *net input* to the  $i$ th PE  $x^i$  given by  $\text{net}_i = \omega_{ij}x^j$ .

For example,

$$\dot{x}^i = -x^i + f_i(\text{net}_i),$$

where  $f_i$  is called *output*, or *activation*, *function*. We apply some input values to the PE so that  $\text{net}_i > 0$ . If the inputs remain for a sufficiently long time, the output value will reach an equilibrium value, when  $\dot{x}^i = 0$ , given by  $x^i = f_i(\text{net}_i)$ . Once the unit has a nonzero output value, removal of the inputs will cause the output to return to zero. If  $\text{net}_i = 0$ , then  $\dot{x}^i = -x^i$ , which means that  $x \rightarrow 0$ .

Second, a general system of coupled ODEs for the *update* of the synaptic weights  $\omega_{ij}$ , i.e., *learning dynamics*, can be written as a generalization of the Oja–Hebb rule, i.e.,

$$\dot{\omega}_{ij} = G_i(\omega_{ij}, x^i, x^i),$$

where  $G_i$  represents the *learning law*; the learning process consists of finding weights that encode the knowledge that we want the system to learn. For most realistic systems, it is not easy to determine a closed-form solution for this system of equations, so the approximative solutions are usually enough.

### 2.5.2 Activation dynamics

Hopfield's graded-response neurons<sup>14</sup> have continuous input-output relation (like nonlinear operational amplifiers) of the form  $V_i = g_i(\lambda u_i)$ , where  $u_i$  denotes the input at  $i$ , a constant  $\lambda$  is called the gain parameter, and  $V_i$  is the output [60]. Usually,  $g_i$  are taken to be sigmoid functions, odd, and monotonically increasing (e.g.,  $g(\cdot) = \frac{1}{2}(1 + \tanh(\cdot))$ ), while discrete Ising spins have  $g_i(u_i) = \text{sgn}_i(u_i)$ . The behavior of the *continuous Hopfield network* is usually described by a set of coupled RC-transient equations

$$C_i \dot{u}_i = I_i + J_{ij} V_j - \frac{u_i}{R_i}, \quad (33)$$

where  $u_i = g^{-1}(V_i)$ ,  $R_i$  and  $C_i$  denote input capacitance and resistance, and  $I_i$  represents an external source.

Using random patterns  $\xi_i^\mu = \pm 1$  with equal probability 1/2, we have the *synaptic*

---

<sup>14</sup>The paradigm for the unsupervised, self-organizing, associative, and recurrent ANN is the discrete Hopfield network (see [59]). Hopfield gives a collection of simple threshold automata, called *formal neurons* by McCulloch and Pitts (see [24, 25]): two-state, 'all-or-none', firing or non-firing units that can be modelled by *Ising spins* (uniaxial magnets)  $\{S_i\}$  such that  $S_i = \pm 1$  (where  $1 = |\uparrow\rangle$  = 'spin up' and  $-1 = |\downarrow\rangle$  = 'spin down'; the label of the neuron is  $i$  and ranges between 1 and the size of the network  $N$ ). The neurons are connected by synapses  $J_{ij}$ .

Firing *patterns*  $\{\xi_i^\mu\}$  represent specific  $S_i$ -*spin configurations*, where the label of the pattern is  $\mu$  and ranges between 1 and  $q$ . Using random patterns  $\xi_i^\mu = \pm 1$  with equal probability 1/2, we have the *synaptic efficacy*  $J_{ij}$  of  $j$ th neuron operating on  $i$ th neuron given by

$$J_{ij} = N^{-1} \xi_i^\mu \xi_j^\mu \equiv N^{-1} \xi_i \cdot \xi_j. \quad (29)$$

*Postsynaptic potential* (PSP) represents an *internal local field*

$$h_i(t) = J_{ij} S_j(t). \quad (30)$$

Now, the *sequential (threshold) dynamics* is defined in the form of discrete equation

$$S_i(t + \Delta t) = \text{sgn}[h_i(t)]. \quad (31)$$

Dynamics (31) is equivalent to the rule that the state of a neuron is changed, or a spin is flipped iff the total network *energy*, given by *Ising Hamiltonian*

$$H_N = -\frac{1}{2} J_{ij} S_i S_j, \quad (32)$$

is lowered [59, ?]. Therefore, the Ising Hamiltonian  $H_N$  represents the monotonically decreasing *Lyapunov function* for the sequential dynamics (31), which converges to a local minimum or ground state of  $H_N$ . This holds for any *symmetric coupling*  $J_{ij} = J_{ji}$  with  $J_{ii} = 0$  and if spin-updating in (31) is asynchronous. In this case the patterns  $\{\xi_i^\mu\}$  after convergence become identical, or very near to, ground states of  $H_N$ , each of them at the bottom of the valley.

efficacy  $J_{ij}$  of  $j$ th neuron operating on  $i$ th neuron given by<sup>15</sup>

$$J_{ij} = N^{-1} \xi_i^\mu \xi_j^\mu \equiv N^{-1} \boldsymbol{\xi}_i \cdot \boldsymbol{\xi}_j. \quad (34)$$

The Hamiltonian of the continuous system (33) is given by

$$H = -\frac{1}{2} J_{ij} V_i V_j + \sum_{i=1}^N R_i^{-1} \int_0^{V_i} dV g^{-1}(V) - I_i V_i. \quad (35)$$

However, according to Hopfield [60] the synapses  $J_{ij}$  retain the form (34) with random patterns  $\xi_i^\mu = \pm 1$  with equal probability  $1/2$ , and the synaptic symmetry  $J_{ij} = J_{ji}$  implies that the continuous Hamiltonian (35) represents a *Lyapunov function* of the system (33), i.e.,  $H$  decreases under the continual neuro-dynamics governed by equation (33) as time proceeds.

### 2.5.3 Hopfield's overlaps

Assuming that the number  $q$  of stored patterns is small compared to the number of neurons, i.e.,  $q/N \rightarrow 0$ , we find that the synapses (34) give rise to a local field of the form

$$h_i = \xi_i^\mu m_\mu, \quad \text{where} \quad (36)$$

$$m_\mu = N^{-1} \xi_i^\mu S_i \quad (37)$$

is the *auto-overlap* (or simply *overlap*)<sup>16</sup> of the network state  $\{S_i\}$  with the pattern  $\{\xi_i^\mu\}$ , measuring the proximity between them. We can see that  $m_\mu = 1$  (like peak-up in auto-correlation) if  $\{S_i\}$  and  $\{\xi_i^\mu\}$  are identical patterns,  $m_\mu = -1$  (like peak-down in autocorrelation) if they are each other's complement, and  $m_\mu = O(1/\sqrt{N})$  if they are uncorrelated (like no-peak in auto-correlation) with each other. Overlaps  $m_\mu$  are related to the Hamming distance  $d_\mu$  between the patterns (the fraction of spins which differ) by  $d_\mu = \frac{1}{2}(1 - m_\mu)$ .

As a pattern  $\xi_i^\mu$  represents (in the simplest case) a specific Ising-spin  $S_i$ -configuration, then  $(\xi_i^\mu)^2 = 1$ . If  $S_i = \xi_i^\mu$  for all  $i$ , then  $m_\mu = 1$ . Conversely, if  $m_\mu = 1$ , then  $S_i = \xi_i^\mu$ . In all other cases  $m_\mu < 1$ , by the Cauchy-Schwartz inequality. If  $\xi_i^\mu$  and  $S_i$  are uncorrelated, we may expect  $m_\mu$  to be of the order of  $N^{-1/2}$ , since the sum consists of  $N$  terms, each

---

<sup>15</sup>More general form of synapses is

$$J_{ij} = N^{-1} Q(\boldsymbol{\xi}_i; \boldsymbol{\xi}_j),$$

for some synaptic kernel  $Q$  on  $\mathbb{R}^n \times \mathbb{R}^n$ . The vector  $\boldsymbol{\xi}_i$  varies as  $i$  travels from 1 to  $N$ , but remains on a corner of the *Hamming hypercube*  $[-1, 1]^q$ .

<sup>16</sup>resembling the auto-correlation function of a time-series, where distinct peaks indicate that the series at the certain time  $t$  is similar to the series at time  $t + \Delta t$

containing a  $\xi_i^\mu$ . On the other hand, if the  $S_i$  are positively correlated with  $\xi_i^\mu$ , then  $m_\mu$  is of the order of unity. So the overlaps give the global information about the network and hence are good order parameters. Also, according to Hopfield [60], the extension to the continual network is straightforward.

Using overlaps, the *Ising Hamiltonian* becomes

$$H_N = -\frac{1}{2}N \sum_{\mu=1}^q m_\mu^2. \quad (38)$$

The similarity between two different patterns  $\xi_i^\mu$  and  $\xi_i^\nu$  is measured by their *mutual overlap* or *cross-overlap*  $m_{\mu\nu}$  (in other parlance it is called *Karhunen–Loeve covariance matrix* (see [25]), which extracts the principal components from a data set)<sup>17</sup>, equal

$$m_{\mu\nu} = N^{-1} \xi_i^\mu \xi_i^\nu. \quad (39)$$

For similar patterns the cross-overlap is close to unity whereas for uncorrelated patterns it is random variable with zero mean and small  $(1/\sqrt{N})$  variance.

The symmetric *Hopfield synaptic matrix*  $J_{ij}$  can be expressed in terms of the cross-overlaps  $m_{\mu\nu}$  as

$$J_{ij} = N^{-1} \xi_i^\mu (m_{\mu\nu})^{-1} \xi_j^\nu = J_{ji}, \quad (40)$$

where  $(m_{\mu\nu})^{-1}$  denotes the *Moore–Penrose pseudoinverse* of the cross-overlap matrix  $m_{\mu\nu}$ .

Besides the Hopfield model, the proposed pattern-overlap picture can be extended to cover some more sophisticated kinds of associative memory, among them [25]:

1. Forgetful memories, characterized by iterative synaptic prescription

$$J_{ij}^{(\mu)} = \phi(\epsilon \xi_i^\mu \xi_j^\mu + J_{ij}^{(\mu-1)}),$$

for some small parameter  $\epsilon$  and some odd function  $\phi$ . If  $\phi(\cdot)$  saturates as  $|\cdot| \rightarrow \infty$ , the memory creates storage capacity for new patterns by forgetting the old ones.

2. Temporal associative memories, which can store and retrieve a sequence of patterns, through synapses

$$N J_{ij} = \xi_i^\mu \xi_j^\mu + \epsilon \sum_{\mu=1}^q \xi_i^{(\mu+1)} \xi_j^\mu, \quad (41)$$

where the second term on the right is associated with a temporal delay, so that one can imagine that the second term ‘pushes’ the neural system through an energy landscape created by the first term.

---

<sup>17</sup>resembling the cross-correlation function of two time-series, with several distinct peaks, indicating that the two series are very similar at each point in time where the peaks occur

### 2.5.4 Overlap dynamics

According to Hopfield [60], the extension of the sequential dynamics  $S_i = \text{sgn}(\sum_{\mu} m_{\mu} \xi_i^{\mu})$  of the network made of the simplest Ising–spin–neurons to the network made of continual graded–response amplifier–neurons, is straightforward using the probabilistic *Glauber dynamics*

$$\text{Prob}\{S_i \mapsto -S_i\} = \frac{1}{2}[1 - \tanh(\beta h_i S_i)], \quad i = 1, \dots, N, \quad (42)$$

where  $\beta$  represents the universal temperature ( $\beta = \frac{1}{k_B T}$ ,  $k_B$  is the normalized Boltzman’s constant and  $k_B T$  has dimension of energy).

Under the Glauber’s dynamics (42), and as  $N \rightarrow \infty$  (transition from the single neurons to the neural field), for time–dependent patterns  $\xi^{\mu}(t) = \xi_{\mu}(t)$ , vector auto–overlaps  $m_{\mu}(t)$ , and tensor cross–overlaps  $m_{\mu\nu}(t)$ , we present the dynamics of overlaps governed by the following nonlinear differential equations [25]

$$\dot{m}_{\mu}(t) = -m_{\mu}(t) + \langle \xi_{\mu}(t) \tanh[\beta m_{\mu}(t) \xi^{\mu}(t)] \rangle, \quad (43)$$

and in the tensor form

$$\dot{m}_{\mu\nu}(t) = -m_{\mu\nu}(t) + \langle \xi_{\mu}(t) \xi_{\nu}(t) \tanh[\beta m_{\mu\nu}(t) \xi^{\mu}(t) \xi^{\nu}(t)] \rangle, \quad (44)$$

where the angular brackets denote an average over the  $q$  patterns  $\xi^{\mu}(t)$ .

The stationary solutions (for any fixed instant of time  $t = \tau$ ) of equations (43) and (44) are given by corresponding fixed–point vector and tensor equations

$$m_{\mu} = \langle \xi_{\mu} \tanh[\beta m_{\mu} \xi^{\mu}] \rangle, \quad \text{and} \quad (45)$$

$$m_{\mu\nu} = \langle \xi_{\mu} \xi_{\nu} \tanh[\beta m_{\mu\nu} \xi^{\mu} \xi^{\nu}] \rangle, \quad (46)$$

respectively.

### 2.5.5 Hebbian learning dynamics

In terms of stochastic feed–forward multi–layer neural networks, the tensorial equation (44) corresponds to the average, general, self–organizing Hebbian neural learning scheme (see [61, 57])

$$\dot{m}_{\mu\nu}(t) = -m_{\mu\nu}(t) + \langle \mathcal{I}_{\mu\nu} \rangle, \quad (47)$$

with random signal *Hebbian innovation*

$$\mathcal{I}_{\mu\nu} = f_{\mu}[\xi^{\mu}(t)] f_{\nu}[\xi^{\nu}(t)] + \sigma_{\mu\nu}(t), \quad (48)$$

where  $\sigma_{\mu\nu}$ , denotes the tensorial, additive, zero–mean, Gaussian white–noise, independent of the main innovation function  $\mathcal{I}_{\mu\nu}$ , while  $f_{\mu,\nu}[\cdot]$  represent the hyperbolic tangent (sigmoid)

neural activation functions. A single-layer Hebbian learning scheme, corresponding to the tensor equation (47), gives

$$\dot{m}_\mu(t) = -m_\mu(t) + \langle \mathcal{I}_\mu \rangle, \quad (49)$$

with the vector innovation

$$\mathcal{I}_\mu = f_\mu[\xi^\mu(t)] + \sigma_\mu(t),$$

where  $\sigma_\mu$ , denotes the vector additive zero-mean Gaussian white-noise, also independent of the main innovation function  $I_\mu$ , while  $f_\mu[\cdot]$  represents the hyperbolic tangent (sigmoid) neural activation function.

If we assume the small absolute value of the average (stochastic) terms, the nonlinear overlap-dynamics equations (43) and (44) can be presented in the form of *weakly-connected neural networks* (see [62]), respectively, as a single-layer network

$$\dot{m}_\mu(t) = -m_\mu(t) + \varepsilon g_\mu(m_\mu, \varepsilon), \quad \varepsilon \ll 1, \quad (50)$$

and a multi-layer network

$$\dot{m}_{\mu\nu}(t) = -m_{\mu\nu}(t) + \varepsilon g_{\mu\nu}(m_{\mu\nu}, \varepsilon), \quad \varepsilon \ll 1, \quad (51)$$

where,  $g_\mu$  and  $g_{\mu\nu}$ , corresponding to the average (bracket) terms in (43) and (44), describe (vector and tensor, respectively) synaptic connections and the ‘small’ parameter  $\varepsilon$  describes their (dimensionless) strength. These weakly-connected neural systems represent  $\varepsilon$ -perturbations of the corresponding linear systems

$$\dot{m}_\mu(t) = -m_\mu(t) \quad \text{and} \quad \dot{m}_{\mu\nu}(t) = -m_{\mu\nu}(t),$$

with exponential maps as solutions

$$m_\mu(t) = m_\mu e^{-t} \quad \text{and} \quad m_{\mu\nu}(t) = m_{\mu\nu} e^{-t},$$

using the stationary (fixed-point) solutions (45, 46) as initial conditions  $m_\mu$  and  $m_{\mu\nu}$ . According to the *Hartman-Grobman theorem* from dynamical systems theory, the weakly-connected systems (50, 51) are topologically equivalent (homeomorphic) to the corresponding linear systems. Therefore the whole analysis for the linear vector and matrix flows can be applied here, with only difference that instead of increasing transients  $e^t$  here we have decreasing (i.e., asymptotically-stable) transients  $e^{-t}$ .

On the other hand, in terms of *synergetics* [63], both nonlinear overlap-dynamics equations (43–44) and Hebbian learning equations (47–48), represent (covariant) *order parameter equations*.

By introducing the scalar quadratic potential fields, dependent on vector and tensor order parameters (overlaps), respectively

$$V(m_\mu) = -\frac{1}{2} \sum_{\mu=1}^q m_\mu^2 \quad \text{and} \quad V(m_{\mu\nu}) = -\frac{1}{2} m_{\mu\nu}^2,$$

we can generalize the overlap–dynamics equations (43–44) to the *stochastic–gradient order parameter equations*, in vector and tensor form, respectively

$$\dot{m}_\mu(t) = -\frac{\partial V(m_\mu)}{\partial m_\mu(t)} + F_\mu(t), \quad (52)$$

and

$$\dot{m}_{\mu\nu}(t) = -\frac{\partial V(m_{\mu\nu})}{\partial m_{\mu\nu}(t)} + F_{\mu\nu}(t). \quad (53)$$

$F_\mu(t)$  in (52) represents a vector fluctuating force, with average (over the stochastic process which produces the fluctuating force  $F_\mu(t)$ )

$$\langle F_\mu(t) \rangle = \langle \xi_\mu(t) \tanh[\beta m_\mu(t) \xi^\mu(t)] \rangle,$$

and variation

$$\langle F_\mu(t) F_\mu(t') \rangle = Q_\mu \delta(t - t'), \quad (54)$$

while  $F_{\mu\nu}(t)$  in (53) represents a tensor fluctuating force, with average (over the stochastic process which produces the fluctuating force  $F_{\mu\nu}(t)$ )

$$\langle F_{\mu\nu}(t) \rangle = \langle \xi_\mu(t) \xi_\nu(t) \tanh[\beta m_{\mu\nu}(t) \xi^\mu(t) \xi^\nu(t)] \rangle,$$

and variation

$$\langle F_{\mu\nu}(t) F_{\mu\nu}(t') \rangle = Q_{\mu\nu} \delta(t - t'). \quad (55)$$

Coefficients  $Q_\mu$  in (54) and  $Q_{\mu\nu}$  in (55) represent strengths of the corresponding stochastic processes, while Dirac  $\delta$ –functions  $\delta(t - t')$  express their short–term memories.

Recall that standard interpretation of synergetics (see [63]) describes the stochastic gradient systems (52–53) as the overdamped motion of (vector and tensor, respectively) representative particles in scalar potential fields  $V(m_\mu)$  and  $V(m_{\mu\nu})$ , subject to fluctuating forces  $F_\mu(t)$  and  $F_{\mu\nu}(t)$ . These particles undergo *non–equilibrium phase transitions* (in the similar way as the magnet undergoes transition from its unmagnetized state into a magnetized state, or a superconductor goes from its normal state into the superconducting state, only occurring now in systems far from thermal equilibrium), and associated phenomena, including a *symmetry breaking instability* and *critical slowing down* (see [63]).

The non–equilibrium phase transitions of vector and tensor order parameters (overlaps)  $m_\mu(t)$  and  $m_{\mu\nu}(t)$ , are in synergetics described in terms of probability distributions  $p(m_\mu, t)$  and  $p(m_{\mu\nu}, t)$ , respectively, defined by corresponding *Fokker–Planck equations*

$$\dot{p}(m_\mu, t) = p(m_\mu, t) + \frac{1}{2} Q_\mu \frac{\partial^2 p(m_\mu, t)}{\partial m_\mu^2},$$

and

$$\dot{p}(m_{\mu\nu}, t) = p(m_{\mu\nu}, t) + \frac{1}{2} Q_{\mu\nu} \frac{\partial^2 p(m_{\mu\nu}, t)}{\partial m_{\mu\nu}^2}.$$

### 2.5.6 Neural attractor dynamics

Recently, *neural attractor dynamics* (NAD) was designed in [22]. based on a discretization for single neurons of Amari's neural field equation (18). The so-called *discrete Amari equation* describes the temporal evolution of the activity of all single neurons considering positive and negative contributions from external input and internal neural interactions. Since only activated neurons can have an impact on other neurons, the neural attractor dynamics is nonlinear, and effects of bi-stability and hysteresis can be used for low-level memory and neural competition. The NAD describes the temporal rate of change of the dynamical variable  $u_i$  of neural activity for all behavioral neurons  $i$ . It is formulated as the following differential equation:

$$\tau \dot{u}_i = -u_i + h + s_i^{\text{beh}} + c_{\text{mot}} \cdot \sigma(m_i) + \alpha_{\text{selfexc},i}^{\text{beh}} + \alpha_{\text{exc},i}^{\text{beh}} - \alpha_{\text{inh},i}^{\text{beh}}, \quad (56)$$

where the system parameters have the following meaning:

$\tau$ , the constant relaxation rate, i.e., the time scale on which the dynamics reacts to changes;

$h$ , the constant negative resting level of neural activation;

$\sigma(\cdot)$ , a sigmoidal function, which maps the value of neural activity onto  $[0, 1]$ , given by

$$\sigma(u) = \frac{1}{1 + e^{-\beta u}},$$

where  $\beta$  (=100) parameterizes the slope of the resulting function;

$s_i^{\text{beh}}$ , the adequate stimulus provided by sensory input of a certain duration;

$u_i$ , activity of behavioral neuron  $i$ , i.e., activity of behavior  $i$ ;

$c_{\text{mot}}$ , a constant for weighting the motivational contribution,  $c_{\text{mot}} < |h|$ ;

$\alpha_{\text{selfexc},i}^{\text{beh}}$  excitatory contribution of neuron  $i$ 's own activity  $u_i$ ;

$\alpha_{\text{exc},i}^{\text{beh}}$ , all excitatory contribution of active neurons connected to neuron  $i$ ;

$\alpha_{\text{inh},i}^{\text{beh}}$ , all inhibitory contribution of active neurons connected to neuron  $i$

$m_i$ , activity of motivational neuron  $i$ , i.e., motivation of behavior  $i$  is in

[22] defined by the following NAD-equation, similar to (56):

$$\tau \dot{m}_i = -m_i + h + s_i^{\text{mot}} + \alpha_{\text{selfexc},i}^{\text{mot}} + \alpha_{\text{exc},i}^{\text{mot}} - \alpha_{\text{inh},i}^{\text{mot}},$$

where

$\alpha_{\text{selfexc},i}^{\text{mot}}$ , excitatory contribution of neuron  $i$ 's own motivation  $m_i$ ;

$\alpha_{\text{exc},i}^{\text{mot}}$ , all excitatory contribution of motivation neurons connected to neuron  $i$ ;

$\alpha_{\text{inh},i}^{\text{mot}}$ , all inhibitory contribution of motivation neurons connected to neuron  $i$ .

In this framework, a nonlinear neural dynamical and control system generates the temporal evolution of behavioral variables, such that desired behaviors are fixed-point attractor solutions while un-desired behaviors are repellers.

This kind of *attractor & repeller dynamics* [23] provides the basis for understanding *cognition*, both natural and artificial [25, 26].



### 2.5.7 Associative bidirectional competitive net

Hopfield recurrent associative memory network can be generalized to get a *bidirectional associative memory* network, the so-called BAM model of Kosko [57]. Here we derive an alternative self-organizing neural net model with competitive *Volterra-Lotka ensemble dynamics* (see [65, 24]).

We start from  $(n + m)$ D linear ODEs, describing two competitive neural ensembles participating in a two-party game,

$$\begin{aligned}\dot{R}^i &= -\alpha_B^j B_j, & R^i(0) &= R_0^i, \\ \dot{B}_j &= -\beta_i^R R^i, & B_j(0) &= B_j^0, \end{aligned} \quad (i = 1, \dots, n; j = 1, \dots, m), \quad (57)$$

where  $R^i = R^i(t)$  and  $B_j = B_j(t)$  respectively represent the numerical strengths of the two neural ensembles at time  $t$ ,  $R_0^i, B_j^0$  are their initial conditions, and  $\alpha_B$  and  $\beta^R$  represent the effective spiking rates (which are either constant, or Poisson random process). In this way, we generate a  $(n + m)$ D smooth manifold  $M$ , a *neural state-space*, and two dynamical objects acting on it: an  $n$ D smooth *vector-field*  $\dot{R}^i$ , and an  $m$ D differential *1-form*  $\dot{B}_j$ . Their dot product  $\dot{R}^i \cdot \dot{B}_j$ , represents a hypothetical *neural outcome*. This is a linear system, with the passive-decay couplings  $\alpha_B^j B_j$  and  $\beta_i^R R^i$ , fully predictable but giving only equilibrium solutions.

Secondly, to incorporate competitive dynamics of Volterra-Lotka style as commonly used in ecological modelling and known to produce a global chaotic attractor [?], we include to each of the neural ensembles a nonlinear competing term depending only on its own units,

$$\begin{aligned}\dot{R}^i &= a^i R^i(1 - b^i R^i) - \alpha_B^j B_j, \\ \dot{B}_j &= c_j B_j(1 - d_j B_j) - \beta_i^R R^i. \end{aligned} \quad (58)$$

Now we have a *competition between the two chaotic attractors*, one for the  $R^i$  and one for the  $B_j$  ensemble, i.e., the two self-organization patterns emerging far-from-equilibrium.

Thirdly, to make this even more realistic, we include the ever-present *noise* in the form of Langevin-type random forces  $F^i = F^i(t)$ , and  $G_j = G_j(t)$ , thus adding the ‘neural heating’, i.e., noise induced entropy growth, to the competitive dynamics

$$\begin{aligned}\dot{R}^i &= a^i R^i(1 - b^i R^i) - \alpha_B^j B_j + F^i, \\ \dot{B}_j &= c_j B_j(1 - d_j B_j) - \beta_i^R R^i + G_j. \end{aligned} \quad (59)$$

Finally, to overcome the deterministic chaos and stochastic noise with an adaptive *brain-like dynamics*, we introduce the *field competition potential*  $V$ , in the scalar form

$$V = -\frac{1}{2}(\omega_i^j R^i B_j + \varepsilon_i^j B_j R^i), \quad (60)$$

where  $\omega_i^j$  and  $\varepsilon_i^j$  represent *synaptic associative-memory* matrices for the  $R^i$  and  $B_j$  ensemble, respectively. From the negative potential  $V$ , we get a *Lyapunov-stable gradient system*  $\dot{R}^i = -\frac{\partial V}{\partial B_j}$ ,  $\dot{B}_j = -\frac{\partial V}{\partial R^i}$ . This robust system, together with the *sigmoidal activation functions*  $S(\cdot) = \tanh(\cdot)$ , and *control inputs*  $u_{OLN}^i = u_{OLN}^i(t)$  and  $v_j^{OLN} = v_j^{OLN}(t)$ , we incorporate into (59) to get the *full neural competitive-associative dynamics*

$$\begin{aligned} \dot{R}^i &= u_{OLN}^i - \alpha_B^j B_j + a^i R^i (1 - b^i R^i) + \omega_i^j S_j(B_j) + F^i, \\ \dot{B}_j &= v_j^{OLN} - \beta_i^R R^i + c_j B_j (1 - d_j B_j) + \varepsilon_i^j S^i(R^i) + G_j, \\ &\text{with initial conditions} \\ R^i(0) &= R_0^i, \quad B_j(0) = B_j^0. \end{aligned} \tag{61}$$

Now, each ensemble learns by trial-and-error from the opposite side. In a standard ANN-fashion, we model this learning on the spot by initially setting the random values to the synaptic matrices  $\omega_i^j$  and  $\varepsilon_i^j$ , and subsequently adjust these values using the standard *Hebbian learning scheme*:

New Value = Old Value + Innovation. In our case it reads:

$$\begin{aligned} \dot{\omega}_i^j &= -\omega_i^j + \Phi_i^j(R^i, B_j), \\ \dot{\varepsilon}_i^j &= -\varepsilon_i^j + \Psi_i^j(B_j, R^i), \end{aligned} \tag{62}$$

with *innovation* given in tensor signal form (generalized from [57])

$$\begin{aligned} \Phi_i^j &= S_j(R^i) S_j(B_j) + \dot{S}_j(R^i) \dot{S}_j(B_j), \\ \Psi_i^j &= S^i(R^i) S^i(B_j) + \dot{S}^i(R^i) \dot{S}^i(B_j), \end{aligned} \tag{63}$$

where terms with overdots, equal  $\dot{S}(\cdot) = 1 - \tanh(\cdot)$ , denote the *signal velocities*.

### 3 Dissipative evolution under the Ricci flow

#### 3.1 Geometrization conjecture

Recall that geometry and topology of smooth surfaces are related by the *Gauss-Bonnet formula* for a closed surface  $\Sigma$  (see, e.g., [6, 30])

$$\frac{1}{2\pi} \iint_{\Sigma} K dA = \chi(\Sigma) = 2 - 2 \text{gen}(\Sigma), \tag{64}$$

where  $dA$  is the area element of a metric  $g$  on  $\Sigma$ ,  $K$  is the Gaussian curvature,  $\chi(\Sigma)$  is the Euler characteristic of  $\Sigma$  and  $\text{gen}(\Sigma)$  is its *genus*, or number of handles, of  $\Sigma$ . Every closed surface  $\Sigma$  admits a metric of constant Gaussian curvature  $K = +1, 0$ , or  $-1$  and

so is uniformized by elliptic, Euclidean, or hyperbolic geometry, which respectively have  $\text{gen}(S^2) = 0$  (sphere),  $\text{gen}(T^2) = 1$  (torus) and  $\text{gen}(\Sigma) > 1$  (torus with several holes). The integral (64) is a *topological invariant* of the surface  $\Sigma$ , always equal to 2 for all topological spheres  $S^2$  (that is, for all closed surfaces without holes that can be continuously deformed from the geometrical sphere) and always equal to 0 for the topological torus  $T^2$  (i.e., for all closed surfaces with one hole or handle).

The general topological framework for the Ricci flow (2) is Thurston's *Geometrization Conjecture* [43], which states that the interior of any compact 3-manifold can be split in an essentially unique way by disjoint embedded 2D spheres  $S^2$  and tori  $T^2$  into pieces and each piece admits one of 8 geometric structures (including (i) the 3D sphere  $S^3$  with constant curvature +1; (ii) the 3D Euclidean space  $\mathbb{R}^3$  with constant curvature 0 and (iii) the 3D hyperbolic space  $\mathbb{H}^3$  with constant curvature  $-1$ ).<sup>18</sup> The geometrization conjecture (which has the Poincaré Conjecture as a special case) would give us a link between the geometry and topology of 3-manifolds, analogous in spirit to the case of 2D surfaces.

In higher dimensions, the Gaussian curvature  $K$  corresponds to the Riemann curvature tensor  $\mathfrak{Rm}$  on a smooth  $n$ -manifold  $M$ , which is in local coordinates on  $M$  denoted by its  $(4, 0)$ -components  $R_{ijkl}$ , or its  $(3, 1)$ -components  $R_{ijk}^l$  (see Appendix, as well as e.g., [6, 30]). The trace (or, contraction) of  $\mathfrak{Rm}$ , using the inverse metric tensor  $g^{ij} = (g_{ij})^{-1}$ , is the Ricci tensor  $\mathfrak{Rc}$ , the 3D curvature tensor, which is in a local coordinate system  $\{x^i\}_{i=1}^n$  defined in an open set  $U \subset M$ , given by

$$R_{ij} = \text{tr}(\mathfrak{Rm}) = g^{kl} R_{ijkl}$$

(using Einstein's summation convention), while the *scalar curvature* is now given by the second contraction of  $\mathfrak{Rm}$  as

$$R = \text{tr}(\mathfrak{Rc}) = g^{ij} R_{ij}.$$

In general, the Ricci flow  $g_{ij}(t)$  is a one-parameter family of Riemannian metrics on a compact  $n$ -manifold  $M$  governed by the equation (2), which has a unique solution for a short time for an arbitrary smooth metric  $g_{ij}$  on  $M$  [36]. If  $\mathfrak{Rc} > 0$  at any local point  $x = \{x^i\}$  on  $M$ , then the Ricci flow (2) contracts the metric  $g_{ij}(t)$  near  $x$ , to the future, while if  $\mathfrak{Rc} < 0$ , then the flow (2) expands  $g_{ij}(t)$  near  $x$ . The solution metric  $g_{ij}(t)$  of the

---

<sup>18</sup>Another five allowed geometric structures are represented by the following examples: (iv) the product  $S^2 \times S^1$ ; (v) the product  $\mathbb{H}^2 \times S^1$  of hyperbolic plane and circle; (vi) a left invariant Riemannian metric on the special linear group  $SL(2, \mathbb{R})$ ; (vii) a left invariant Riemannian metric on the solvable Poincaré-Lorentz group  $E(1, 1)$ , which consists of rigid motions of a  $(1 + 1)$ -dimensional space-time provided with the flat metric  $dt^2 - dx^2$ ; (viii) a left invariant metric on the nilpotent Heisenberg group, consisting of  $3 \times 3$  matrices of the form

$$\begin{bmatrix} 1 & * & * \\ 0 & 1 & * \\ 0 & 0 & 1 \end{bmatrix}.$$
 In each case, the universal covering of the indicated manifold provides a canonical model for the corresponding geometry [37].

Ricci flow equation (2) shrinks in positive Ricci curvature direction while it expands in the negative Ricci curvature direction, because of the minus sign in the front of the Ricci tensor  $R_{ij}$ . In particular, in 2D, on a sphere  $S^2$ , any metric of positive Gaussian curvature will shrink to a point in finite time. At a general point, there will be directions of positive and negative Ricci curvature along which the metric will locally contract or expand (see [38]). In 3D, if a simply-connected compact 3-manifold  $M$  has a Riemannian metric  $g_{ij}$  with positive Ricci curvature then it is diffeomorphic to the 3-sphere  $S^3$  [36].

### 3.2 Heat-type evolution of curvatures and volumes

All three Riemannian curvatures ( $R$ ,  $\mathfrak{Rc}$  and  $\mathfrak{Rm}$ ), as well as the associated volume forms, *evolve* during the Ricci flow (2).

The Ricci flow evolution equation (2) for the metric tensor  $g_{ij}$  implies the evolution equation for the Riemann curvature tensor  $\mathfrak{Rm}$ ,

$$\partial_t \mathfrak{Rm} = \Delta \mathfrak{Rm} + Q_n, \quad (65)$$

where  $Q_n$  is a certain quadratic expression of the Riemann curvatures. From the general  $n$ -curvature expression (65) we have two special cases important for geometric evolution:<sup>19</sup>

- The 3D evolution equation for the Ricci curvature tensor  $\mathfrak{Rc}$  on any 3-manifold  $M$ ,

$$\partial_t \mathfrak{Rc} = \Delta \mathfrak{Rc} + Q_3, \quad (66)$$

where  $Q_3$  is a certain quadratic expression of the Ricci curvatures; and

- The 2D evolution equation for the scalar surface curvature  $R$ ,

$$\partial_t R = \Delta R + 2|\mathfrak{Rc}|^2, \quad (67)$$

which holds both on any 3-manifold  $M$  and on its 2D boundary surface  $\partial M$ . Therefore, by the *maximum principle*, the minimum of  $R$  is non-decreasing along the flow  $g(t)$ , both on  $M$  and on  $\partial M$  (see [34]).

---

<sup>19</sup>By expanding the maximum principle for tensors, Hamilton proved that Ricci flow  $g(t)$  given by (2) preserves the positivity of the Ricci tensor  $\mathfrak{Rc}$  in 3D (as well as of the Riemann curvature tensor  $\mathfrak{Rm}$  in all dimensions); moreover, the eigenvalues of the Ricci tensor in 3D (and of the curvature operator  $\mathfrak{Rm}$  in 4D) are getting pinched point-wisely as the curvature is getting large [36, 39]. This observation allowed him to prove the convergence results: the evolving metrics (on a compact manifold) of positive Ricci curvature in 3D (or positive Riemann curvature in 4D) converge, modulo scaling, to metrics of constant positive curvature.

However, without assumptions on curvature, the long time behavior of the metric evolving by Ricci flow may be more complicated [34]. In particular, as  $t$  approaches some finite time  $T$ , the curvatures may become arbitrarily large in some region while staying bounded in its complement. On the other hand, Hamilton [40] discovered a remarkable property of solutions with nonnegative curvature tensor  $\mathfrak{Rm}$  in arbitrary dimension, called the *differential Harnack inequality*, which allows, in particular, to compare the curvatures of the solution of (2) at different points and different times.

Let us now see in detail how various related geometric quantities evolve given the short-time solution of the Ricci flow equation (2) on any 3-manifold  $M$ . Let us first calculate the *variation formulas* for the Christoffel symbols and curvature tensors on  $M$  and then the corresponding evolution equations (see [36, 44, 45]). If  $g(s)$  is a one-parameter family of metrics on  $M$  with

$$\partial_s g_{ij} = v_{ij},$$

then the variation of the Christoffel symbols  $\Gamma_{ij}^k$  on  $M$  is given by

$$\partial_s \Gamma_{ij}^k = \frac{1}{2} g^{kl} (\nabla_i v_{jl} + \nabla_j v_{il} - \nabla_l v_{ij}), \quad (68)$$

from which follows the evolution of the Christoffel symbols  $\Gamma_{ij}^k$  under the Ricci flow  $g(t)$  on  $M$  given by (2),

$$\partial_t \Gamma_{ij}^k = -g^{kl} (\nabla_i R_{jl} + \nabla_j R_{il} - \nabla_l R_{ij}).$$

From (68) we calculate the variation of the Ricci tensor  $R_{ij}$  on  $M$  as

$$\partial_s R_{ij} = \nabla_m (\partial_s \Gamma_{ij}^m) - \nabla_i (\partial_s \Gamma_{mj}^m), \quad (69)$$

and the variation of scalar curvature  $R$  on  $M$  by

$$\partial_s R = -\Delta V + \operatorname{div}(\operatorname{div} v) - \langle v, \mathfrak{R} \rangle, \quad (70)$$

where  $V = g^{ij} v_{ij} = \operatorname{tr}(v)$  is the trace of  $v = (v_{ij})$ .

If a 3-manifold  $M$  is oriented, then the *volume* 3-form on  $M$  is given, in a positively oriented local coordinate system  $\{x^i\} \in U \subset M$ , by<sup>20</sup>

$$d\mu = \sqrt{\det(g_{ij})} dx^1 \wedge dx^2 \wedge dx^3. \quad (71)$$

If  $\partial_s g_{ij} = v_{ij}$ , then

$$\partial_s d\mu = \frac{1}{2} V d\mu.$$

The evolution of the volume form  $d\mu$  under the Ricci flow  $g(t)$  on  $M$  is given by the exponential decay/growth relation with the scalar curvature  $R$  as the rate constant,

$$\partial_t d\mu = -R d\mu, \quad (72)$$

which gives an exponential decay for  $R > 0$  (elliptic geometry) and exponential growth for  $R < 0$  (hyperbolic geometry). The elementary volume evolution (72) implies the integral form of the exponential relation for the total 3-volume

$$\operatorname{vol}(g) = \int_M d\mu,$$

---

<sup>20</sup>Extension to higher-dimensional Riemannian manifolds is obvious [30]; also, for related volume forms on symplectic manifolds, see [31]

in the form

$$\partial_t \text{vol}(g(t)) = - \int_M R d\mu,$$

which again gives an exponential decay for elliptic  $R > 0$  and exponential growth for hyperbolic  $R < 0$ .

Since the 3-volume is not constant and sometimes we would like to prevent the solution from shrinking to a point on  $M$  (elliptic case) or expanding to infinity (hyperbolic case), we can also consider the *normalized Ricci flow* on  $M$  (see Figure 1 as well as ref. [44]):

$$\partial_t \hat{g}_{ij} = -2\hat{R}_{ij} + \frac{2}{n}\hat{r}\hat{g}_{ij}, \quad (73)$$

where

$$\hat{r} = \text{vol}(\hat{g})^{-1} \int_M \hat{R} d\mu$$

is the average scalar curvature on  $M$ . We then have the *volume conservation law*:

$$\partial_t \text{vol}(\hat{g}(t)) = 0.$$

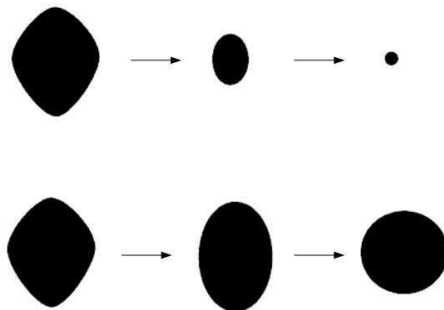


Figure 1: An example of Ricci flow normalization: unnormalized flow (up) and normalized flow (down).

To study the long-time existence of the normalized Ricci flow (73) on any 3-manifold  $M$ , it is important to know what kind of curvature conditions are preserved under the equation. In general, the Ricci flow  $g(t)$  on  $M$  tends to preserve some kind of positivity of curvatures. For example, positive scalar curvature  $R$  is preserved both on  $M$  and on its boundary  $\partial M$ . This follows from applying the maximum principle to the evolution equation (67) for scalar curvature  $R$  both on  $M$  and on  $\partial M$ . Also, positive Ricci curvature is preserved under the Ricci flow on  $M$ . (This is a special feature of 3D and is related to

the fact that the Riemann curvature tensor may be recovered algebraically from the Ricci tensor and the metric in 3D [44].)

In particular, we have the following result (see [41]) for 2-surfaces  $\partial M$ : Let  $\partial M$  be a closed 2-surface. Then for any initial 2D metric  $g_0$  on  $\partial M$ , the solution to the normalized Ricci flow (73) on  $\partial M$  exists for all time. Moreover, (i) If the Euler characteristic of  $\partial M$  is non-positive, then the solution metric  $g(t)$  on  $\partial M$  converges to a constant curvature metric as  $t \rightarrow \infty$ ; and (ii) If the scalar curvature  $R$  of the initial metric  $g_0$  is positive, then the solution metric  $g(t)$  on  $\partial M$  converges to a positive constant curvature metric as  $t \rightarrow \infty$ . (For surfaces with non-positive Euler characteristic, the proof is based primarily on maximum principle estimates for the scalar curvature.)

The negative flow of the total 3-volume  $\text{vol}(g(t))$  is the *Einstein–Hilbert functional*, given by (see [56, 44, 38])

$$E(g) = \int_M R d\mu = -\partial_t \text{vol}(g(t)).$$

If we put  $\partial_s g_{ij} = v_{ij}$ , we have

$$\begin{aligned} \partial_s E(g) &= \int_M \left( -\Delta V + \text{div}(\text{div } v) - \langle v, \mathfrak{Rc} \rangle + \frac{1}{2} R V \right) d\mu \\ &= \int_M \left\langle v, \frac{1}{2} R g_{ij} - R_{ij} \right\rangle d\mu, \end{aligned}$$

so the critical points of  $E(g)$  satisfy *Einstein's equation*

$$\frac{1}{2} R g_{ij} - R_{ij} = 0.$$

The gradient flow of  $E(g)$  on  $M$ , given by

$$\partial_t g_{ij} = 2(\nabla E(g))_{ij} = R g_{ij} - 2R_{ij},$$

is almost the Ricci flow (2). Thus, Einstein metrics are the fixed points of the Ricci flow  $g(t)$  on  $M$ .<sup>21</sup>

Let  $\Delta$  denote the Laplacian acting on functions on any 3-manifold  $M$ , which is in local coordinates  $\{x^i\} \in U \subset M$  given by

$$\Delta = g^{ij} \nabla_i \nabla_j = g^{ij} \left( \partial_{ij} - \Gamma_{ij}^k \partial_k \right).$$

---

<sup>21</sup>In 3D manifolds, Einstein metrics are metrics with constant curvature. However, along the way, the deformation will encounter singularities. The major question, resolved by Perelman, was how to find a way to describe all possible singularities.

For any smooth function  $f$  on  $M$  we have [36, 45]

$$\begin{aligned}\Delta \nabla_i f &= \nabla_i \Delta f + R_{ij} \nabla_j f, & \text{and} \\ \Delta |\nabla f|^2 &= 2|\nabla_i \nabla_j f|^2 + 2R_{ij} \nabla_i f \nabla_j f + 2\nabla_i f \nabla_i \Delta f.\end{aligned}$$

From this it follows that if we have

$$\begin{aligned}\mathfrak{Rc} &\geq 0, & \Delta f &\equiv 0, & |\nabla f| &\equiv 1, & \text{then} \\ \nabla \nabla f &\equiv 0 & \text{and} & \mathfrak{Rc}(\nabla f, \nabla f) &\equiv 0.\end{aligned}$$

Using  $\Delta$ , we can write the linear heat equation on  $M$  as

$$\partial_t u = \Delta u,$$

where  $u$  is the temperature. In particular, the Laplacian acting on functions with respect to  $g(t)$  will be denoted by  $\Delta_{g(t)}$ . If  $(M, g(t))$  is a solution to the Ricci flow equation (2), then we have

$$\partial_t \Delta_{g(t)} = 2R_{ij} \nabla_i \nabla_j.$$

Now, the evolution equation (67) for the scalar curvature  $R$  under the Ricci flow (2) follows from (70). Using equation (83) from Appendix, we have:

$$\operatorname{div}(\mathfrak{Rc}) = \frac{1}{2} \nabla R, \quad \text{so that} \quad \operatorname{div}(\operatorname{div}(\mathfrak{Rc})) = \frac{1}{2} \Delta R,$$

showing again that the scalar curvature  $R$  satisfies a heat-type equation with a quadratic nonlinearity both on a 3-manifold  $M$  and on its boundary 2-surface  $\partial M$ .

Next we will find the exact form of the evolution equation (66) for the Ricci tensor  $\mathfrak{Rc}$  under the Ricci flow  $g(t)$  given by (2) on any 3-manifold  $M$ . (Note that in higher dimensions, the appropriate formula would involve the whole Riemann curvature tensor  $\mathfrak{Rm}$ .) In general, given a variation  $\partial_s g_{ij} = v_{ij}$ , from (69) we get

$$\partial_s R_{ij} = \frac{1}{2} (\Delta_L v_{ij} + \nabla_i \nabla_j V - \nabla_i (\operatorname{div} v)_j - \nabla_j (\operatorname{div} v)_i),$$

where  $\Delta_L$  denotes the so-called Lichnerowicz Laplacian (which depends on  $\mathfrak{Rm}$ ) (see [36, 45]). Since

$$\nabla_i \nabla_j R - \nabla_i (\operatorname{div}(\mathfrak{Rc}))_j - \nabla_j (\operatorname{div}(\mathfrak{Rc}))_i = 0,$$

by (83) (after some algebra) we get that under the Ricci flow (2) the evolution equation for the Ricci tensor  $\mathfrak{Rc}$  on  $M$  is

$$\partial_t R_{ij} = \Delta R_{ij} + 3R R_{ij} - 6R_{im} R_{jm} + (2|\mathfrak{Rc}|^2 - R^2) g_{ij}.$$



So, just as in case of the evolution (67) of the scalar curvature  $\partial_t R$  (both on  $M$  and on its boundary  $\partial M$ ), we get a heat-type evolution equation with a quadratic nonlinearity for  $\partial_t R_{ij}$ , which means that positive Ricci curvature ( $\mathfrak{R}\mathfrak{c} > 0$ ) of elliptic 3-geometry is preserved under the Ricci flow  $g(t)$  on  $M$ .

More generally, we have the following result for 3-manifolds (see [36]): Let  $(M, g_0)$  be a compact Riemannian 3-manifold with positive Ricci curvature  $\mathfrak{R}\mathfrak{c}$ . Then there exists a unique solution to the normalized Ricci flow  $g(t)$  on  $M$  with  $g(0) = g_0$  for all time and the metrics  $g(t)$  converge exponentially fast to a constant positive sectional curvature metric  $g_\infty$  on  $M$ . In particular,  $M$  is diffeomorphic to a 3D sphere  $S^3$ . (As a consequence, such an MST 3-manifold  $M$  is necessarily diffeomorphic to a quotient of the 3-sphere by a finite group of isometries. It follows that given any homotopy 3-sphere, if one can show that it admits a metric with positive Ricci curvature, then the Poincaré Conjecture would follow [44].) In particular, compact and closed 3-manifolds which admit a non-singular solution can also be decomposed into geometric pieces [42].

### 3.3 Dissipative solitons

In general, dissipative solitons (DSs) are stable solitary localized structures that arise in nonlinear spatially extended dissipative systems due to mechanisms of self-organization. They can be considered as an extension of the classical soliton concept in conservative systems. Apart from aspects similar to the behavior of classical particles like the formation of bound states, DSs exhibit entirely nonclassical behavior – e.g., scattering, generation and annihilation – all without the constraints of energy or momentum conservation. The excitation of internal degrees of freedom may result in a dynamically stabilized intrinsic speed, or periodic oscillations of the shape.

In particular, stationary DSs are generated by production of material in the center of the DSs, diffusive transport into the tails and depletion of material in the tails. A propagating pulse arises from production in the leading and depletion in the trailing end. Among other effects, one finds periodic oscillations of DSs, the so-called ‘breathing’ dissipative solitons [8].

DSs in many different systems show universal particle-like properties. To understand and describe the latter, one may try to derive ‘particle equations’ for slowly varying order parameters like position, velocity or amplitude of the DSs by adiabatically eliminating all fast variables in the field description. This technique is known from linear systems, however mathematical problems arise from the nonlinear models due to a coupling of fast and slow modes [3].

Similar to low-dimensional dynamic systems, for supercritical bifurcations of stationary DSs one finds characteristic normal forms essentially depending on the symmetries of the system; e.g., for a transition from a symmetric stationary to an intrinsically propagat-

ing DS one finds the Pitchfork normal form for the DS-velocity  $\mathbf{v}$  [4],

$$\dot{\mathbf{v}} = (\sigma - \sigma_0)\mathbf{v} - |\mathbf{v}|^2\mathbf{v}$$

where  $\sigma$  represents the bifurcation parameter and  $\sigma_0$  the bifurcation point. For a bifurcation to a ‘breathing’ DS, one finds the Hopf normal form

$$\dot{A} = (\sigma - \sigma_0)A - |A|^2 A$$

for the amplitude  $A$  of the oscillation. Note that the above problems do not arise for classical solitons as inverse scattering theory yields complete analytical solutions [8].

### 3.4 Ricci breathers and solitons

Closely related to dissipative solitons (see subsection 2) are the so-called *breathers*, solitonic structures given by localized periodic solutions of some nonlinear soliton PDEs, including the exactly solvable sine-Gordon equation<sup>22</sup> and the focusing nonlinear Schrödinger equation.<sup>23</sup>

A metric  $g_{ij}(t)$  evolving by the Ricci flow  $g(t)$  given by (2) on any 3-manifold  $M$  is called a *Ricci breather*, if for some  $t_1 < t_2$  and  $\alpha > 0$  the metrics  $\alpha g_{ij}(t_1)$  and  $g_{ij}(t_2)$  differ only by a diffeomorphism; the cases  $\alpha = 1, \alpha < 1, \alpha > 1$  correspond to steady, shrinking and expanding breathers, respectively. Trivial breathers on  $M$ , for which the metrics  $g_{ij}(t_1)$  and  $g_{ij}(t_2)$  differ only by diffeomorphism and scaling for each pair of  $t_1$  and  $t_2$ , are called *Ricci solitons*. Thus, if one considers Ricci flow as a dynamical system on the space of Riemannian metrics modulo diffeomorphism and scaling, then breathers

---

<sup>22</sup>An exact solution  $u = u(x, t)$  of the (1+1)D sine-Gordon equation

$$\frac{\partial^2 u}{\partial t^2} = \frac{\partial^2 u}{\partial x^2} - \sin u,$$

is [50]

$$u = 4 \arctan \left( \frac{\sqrt{1 - \omega^2} \cos(\omega t)}{\omega \cosh(\sqrt{1 - \omega^2} x)} \right),$$

which, for  $\omega < 1$ , is periodic in time  $t$  and decays exponentially when moving away from  $x = 0$ .

<sup>23</sup>The focusing nonlinear Schrödinger equation is the dispersive complex-valued (1+1)D PDE [51],

$$i \frac{\partial u}{\partial t} + \frac{\partial^2 u}{\partial x^2} + |u|^2 u = 0, \quad (i = \sqrt{-1}, u = u(x, t))$$

with a breather solution of the form:

$$u = \left( \frac{2b^2 \cosh(\theta) + 2ib\sqrt{2-b^2} \sinh(\theta)}{2 \cosh(\theta) - \sqrt{2}\sqrt{2-b^2} \cos(ax)} - 1 \right) a \exp(ia^2 t) \quad \text{with} \quad \theta = a^2 b \sqrt{2-b^2} t,$$

which gives breathers periodic in space  $x$  and approaching the uniform value  $a$  when moving away from the focus time  $t = 0$ .

and solitons correspond to periodic orbits and fixed points respectively. At each time the Ricci soliton metric satisfies on  $M$  an equation of the form [34]

$$R_{ij} + cg_{ij} + \nabla_i b_j + \nabla_j b_i = 0,$$

where  $c$  is a number and  $b_i$  is a 1-form; in particular, when  $b_i = \frac{1}{2}\nabla_i a$  for some function  $a$  on  $M$ , we get a gradient Ricci soliton. An important example of a gradient shrinking soliton is the *Gaussian soliton*, for which the metric  $g_{ij}$  is just the Euclidean metric on  $\mathbb{R}^3$ ,  $c = 1$  and  $a = -|x|^2/2$ .

### 3.5 Heat equation and Ricci entropy

Given a  $C^2$  function  $u : M \rightarrow \mathbb{R}$  on a Riemannian 3-manifold  $M$ , its Laplacian is defined in local coordinates  $\{x^i\} \in U \subset M$  to be

$$\Delta u = \text{tr}_g (\nabla^2 u) = g^{ij} \nabla_i \nabla_j u,$$

where  $\nabla_i$  is its associated covariant derivative (Levi-Civita connection, see Appendix). We say that a  $C^2$  function  $u : M \times [0, T) \rightarrow \mathbb{R}$ , where  $T \in (0, \infty]$ , is a solution to the heat equation on  $M$  if

$$\partial_t u = \Delta u. \tag{74}$$

One of the most important properties satisfied by the heat equation is the *maximum principle*, which says that for any smooth solution to the heat equation, whatever point-wise bounds hold at  $t = 0$  also hold for  $t > 0$  [44]. More precisely, we can state: Let  $u : M \times [0, T) \rightarrow \mathbb{R}$  be a  $C^2$  solution to the heat equation (74) on a complete Riemannian 3-manifold  $M$ . If  $C_1 \leq u(x, 0) \leq C_2$  for all  $x \in M$ , for some constants  $C_1, C_2 \in \mathbb{R}$ , then  $C_1 \leq u(x, t) \leq C_2$  for all  $x \in M$  and  $t \in [0, T)$ . This property exhibits the smoothing behavior of the heat equation (74) on  $M$ .

Now, consider Perelman's *entropy functional* [34] on any 3-manifold  $M$

$$\mathcal{F} = \int_M (R + |\nabla f|^2) e^{-f} d\mu \tag{75}$$

for a Riemannian metric  $g_{ij}$  and a (temperature-like) scalar function  $f$  on a closed 3-manifold  $M$ , where  $d\mu$  is the volume 3-form (71). During the Ricci flow (2),  $\mathcal{F}$  evolves on  $M$  as

$$\partial_t \mathcal{F} = 2 \int_M |R_{ij} + \nabla_i \nabla_j f|^2 e^{-f} d\mu. \tag{76}$$

Now, define  $\lambda(g_{ij}) = \inf \mathcal{F}(g_{ij}, f)$ , where infimum is taken over all smooth  $f$ , satisfying

$$\int_M e^{-f} d\mu = 1. \tag{77}$$

$\lambda(g_{ij})$  is the lowest eigenvalue of the operator  $-4\Delta + R$ . Then the entropy evolution formula (76) implies that  $\lambda(g_{ij}(t))$  is nondecreasing in  $t$ , and moreover, if  $\lambda(t_1) = \lambda(t_2)$ , then for  $t \in [t_1, t_2]$  we have  $R_{ij} + \nabla_i \nabla_j f = 0$  for  $f$  which minimizes  $\mathcal{F}$  on  $M$  [34]. Thus a steady breather on  $M$  is necessarily a steady soliton.

If we define the conjugate *heat operator* on  $M$  as

$$\square^* = -\partial/\partial t - \Delta + R$$

then we have the *conjugate heat equation*<sup>24</sup> [34]

$$\square^* u = 0. \tag{79}$$

The entropy functional (75) is nondecreasing under the following coupled *Ricci-heat flow* on  $M$  [49]

$$\begin{aligned} \partial_t g_{ij} &= -2R_{ij}, \\ \partial_t u &= -\Delta u - \frac{|\nabla u|^2}{u} + \frac{R}{2}u, \end{aligned} \tag{80}$$

where the modified conjugate heat equation (80) ensures

$$\int_M u^2 d\mu = 1$$

---

<sup>24</sup>In [34] Perelman stated a differential Li–Yau–Hamilton (LYH) type inequality [46] for the fundamental solution  $u = u(x, t)$  of the conjugate heat equation (79) on a closed  $n$ -manifold  $M$  evolving by the Ricci flow (2). Let  $p \in M$  and

$$u = (4\pi\tau)^{-\frac{n}{2}} e^{-f}$$

be the fundamental solution of the conjugate heat equation in  $M \times (0, T)$ ,

$$\square^* u = 0, \quad \text{or} \quad \partial_t u + \Delta u = Ru,$$

where  $\tau = T - t$  and  $R = R(\cdot, t)$  is the scalar curvature of  $M$  with respect to the metric  $g(t)$  with  $\lim_{t \nearrow T} u = \delta_p$  (in the distribution sense), where  $\delta_p$  is the delta-mass at  $p$ . Let

$$v = [\tau(2\Delta f - |\nabla f|^2 + R) + f - n]u,$$

where  $\tau = T - t$ . Then we have a differential LYH-type inequality

$$v(x, t) \leq 0 \quad \text{in } M \times (0, T). \tag{78}$$

This result was used by Perelman to give a proof of the *pseudolocality theorem* [34] which roughly said that almost Euclidean regions of large curvature in closed manifold with metric evolving by Ricci flow  $g(t)$  given by (2) remain localized.

In particular, let  $(M, g(t))$ ,  $0 \leq t \leq T$ ,  $\partial M \neq \emptyset$ , be a compact 3-manifold with metric  $g(t)$  evolving by the Ricci flow  $g(t)$  given by (2) such that the second fundamental form of the surface  $\partial M$  with respect to the unit outward normal  $\partial/\partial\nu$  of  $\partial M$  is uniformly bounded below on  $\partial M \times [0, T]$ . A global Li–Yau gradient estimate [47] for the solution of the generalized conjugate heat equation was proved in [46] (using a variation of the method of P. Li and S.T. Yau, [47]) on such a manifold with Neumann boundary condition.

to be preserved by the Ricci flow  $g(t)$  on  $M$ . If we define  $u = e^{-\frac{f}{2}}$ , then (80) is equivalent to  $f$ -evolution equation on  $M$ ,

$$\partial_t f = -\Delta f + |\nabla f|^2 - R,$$

which instead preserves (77).

Note that in the related context of Riemannian gravitation theory, the so-called *gravitational entropy* is embedded in the Weyl curvature  $(4, 0)$ -tensor  $\mathfrak{W}$ , which is the traceless component of the Riemann curvature tensor  $\mathfrak{Rm}$  (i.e.,  $\mathfrak{Rm}$  with the Ricci tensor  $\mathfrak{Rc}$  removed),

$$\mathfrak{W} = \mathfrak{Rm} - f(R_{ij}g_{ij}),$$

where  $f(R_{ij}g_{ij})$  is a certain linear function of  $R_{ij}$  and  $g_{ij}$ .<sup>25</sup> According to Penrose's *Weyl curvature hypothesis*, the entire *history of a closed universe* starts from a uniform low-entropy Big Bang with zero Weyl curvature tensor of the cosmological gravitational field and ends with a high-entropy Big Crunch, representing the congealing of many black holes, with Weyl tensor approaching infinity (see [33, 32]).

### 3.6 Thermodynamic analogy

Perelman's functional  $\mathcal{F}$  is analogous to negative entropy [34]. Recall that thermodynamic *partition function* for a generic canonical ensemble at temperature  $\beta^{-1}$  is given by

$$Z = \int e^{-\beta E} d\omega(E), \quad (81)$$

where  $\omega(E)$  is a 'density measure', which does not depend on  $\beta$ . From it, the *average energy* is given by

$$\langle E \rangle = -\partial_\beta \ln Z,$$

the *entropy* is

$$S = \beta \langle E \rangle + \ln Z,$$

and the *fluctuation* is

$$\sigma = \langle (E - \langle E \rangle)^2 \rangle = \partial_{\beta^2} \ln Z.$$

If we now fix a closed 3-manifold  $M$  with a probability measure  $m$  and a metric  $g_{ij}(\tau)$  that depends on the temperature  $\tau$ , then according to equation

$$\partial_\tau g_{ij} = 2(R_{ij} + \nabla_i \nabla_j f),$$

---

<sup>25</sup>In local coordinates of an  $n$ -manifold  $M$ , the conformal Weyl tensor  $\mathfrak{W}$  is given by

$$W_{ijkl} = R_{ijkl} - \frac{2}{n-2}(g_{i[k}R_{l]j} - g_{j[k}R_{l]i}) + \frac{2}{(n-1)(n-2)}R g_{i[k}g_{l]j},$$

where  $[\cdot]$  denotes the antisymmetric part of a tensor.

the partition function (81) is given by

$$\ln Z = \int (-f + \frac{n}{2}) dm. \quad (82)$$

From (82) we get (see [34])

$$\begin{aligned} \langle E \rangle &= -\tau^2 \int_M (R + |\nabla f|^2 - \frac{n}{2\tau}) dm, \\ S &= - \int_M (\tau(R + |\nabla f|^2) + f - n) dm, \\ \sigma &= 2\tau^4 \int_M |R_{ij} + \nabla_i \nabla_j f - \frac{1}{2\tau} g_{ij}|^2 dm, \end{aligned}$$

where

$$dm = u dV, \quad u = (4\pi\tau)^{-\frac{n}{2}} e^{-f}.$$

From the above formulas, we see that the fluctuation  $\sigma$  is nonnegative; it vanishes only on a gradient shrinking soliton.  $\langle E \rangle$  is nonnegative as well, whenever the flow exists for all sufficiently small  $\tau > 0$ . Furthermore, if the heat function  $u$ : (a) tends to a  $\delta$ -function as  $\tau \rightarrow 0$ , or (b) is a limit of a sequence of partial heat functions  $u_i$ , such that each  $u_i$  tends to a  $\delta$ -function as  $\tau \rightarrow \tau_i > 0$ , and  $\tau_i \rightarrow 0$ , then the entropy  $S$  is also nonnegative. In case (a), all the quantities  $\langle E \rangle, S, \sigma$  tend to zero as  $\tau \rightarrow 0$ , while in case (b), which may be interesting if  $g_{ij}(\tau)$  becomes singular at  $\tau = 0$ , the entropy  $S$  may tend to a positive limit.

## 4 Appendix: Riemann and Ricci curvatures on a smooth $n$ -manifold

Recall that proper differentiation of vector and tensor fields on a smooth Riemannian  $n$ -manifold is performed using the *Levi-Civita covariant derivative* (see, e.g., [6, 30]). Formally, let  $M$  be a Riemannian  $n$ -manifold with the tangent bundle  $TM$  and a local coordinate system  $\{x^i\}_{i=1}^n$  defined in an open set  $U \subset M$ . The covariant derivative operator,  $\nabla_X : C^\infty(TM) \rightarrow C^\infty(TM)$ , is the unique linear map such that for any vector fields  $X, Y, Z$ , constant  $c$ , and function  $f$  the following properties are valid:

$$\begin{aligned} \nabla_{X+cY} &= \nabla_X + c\nabla_Y, \\ \nabla_X(Y + fZ) &= \nabla_X Y + (Xf)Z + f\nabla_X Z, \\ \nabla_X Y - \nabla_Y X &= [X, Y], \end{aligned}$$

where  $[X, Y]$  is the Lie bracket of  $X$  and  $Y$  (see, e.g., [31]). In local coordinates, the metric  $g$  is defined for any orthonormal basis  $(\partial_i = \partial_{x^i})$  in  $U \subset M$  by

$$g_{ij} = g(\partial_i, \partial_j) = \delta_{ij}, \quad \partial_k g_{ij} = 0.$$

Then the affine *Levi-Civita connection* is defined on  $M$  by

$$\nabla_{\partial_i} \partial_j = \Gamma_{ij}^k \partial_k, \quad \text{where}$$

$$\Gamma_{ij}^k = \frac{1}{2} g^{kl} (\partial_i g_{jl} + \partial_j g_{il} - \partial_l g_{ij})$$

are the (second-order) *Christoffel symbols*.

Now, using the covariant derivative operator  $\nabla_X$  we can define the *Riemann curvature*  $(3, 1)$ -tensor  $\mathfrak{Rm}$  by (see, e.g., [6, 30])

$$\mathfrak{Rm}(X, Y)Z = \nabla_X \nabla_Y Z - \nabla_Y \nabla_X Z - \nabla_{[X, Y]} Z.$$

$\mathfrak{Rm}$  measures the curvature of the manifold by expressing how noncommutative covariant differentiation is. The  $(3, 1)$ -components  $R_{ijk}^l$  of  $\mathfrak{Rm}$  are defined in  $U \subset M$  by

$$\begin{aligned} \mathfrak{Rm}(\partial_i, \partial_j) \partial_k &= R_{ijk}^l \partial_l, \quad \text{which expands as [56],} \\ R_{ijk}^l &= \partial_i \Gamma_{jk}^l - \partial_j \Gamma_{ik}^l + \Gamma_{jk}^m \Gamma_{im}^l - \Gamma_{ik}^m \Gamma_{jm}^l. \end{aligned}$$

Also, the Riemann  $(4, 0)$ -tensor  $R_{ijkl} = g_{lm} R_{ijk}^m$  is defined as the  $g$ -based inner product on  $M$ ,

$$R_{ijkl} = \langle \mathfrak{Rm}(\partial_i, \partial_j) \partial_k, \partial_l \rangle.$$

The first and second Bianchi identities for the Riemann  $(4, 0)$ -tensor  $R_{ijkl}$  hold,

$$\begin{aligned} R_{ijkl} + R_{jkil} + R_{kijl} &= 0, \\ \nabla_i R_{jklm} + \nabla_j R_{kilm} + \nabla_k R_{ijlm} &= 0, \end{aligned}$$

while the twice contracted second Bianchi identity reads

$$2\nabla_j R_{ij} = \nabla_i R. \tag{83}$$

The  $(0, 2)$  *Ricci tensor*  $\mathfrak{Rc}$  is the trace of the Riemann  $(3, 1)$ -tensor  $\mathfrak{Rm}$ ,

$$\mathfrak{Rc}(Y, Z) + \text{tr}(X \rightarrow \mathfrak{Rm}(X, Y)Z),$$

so that

$$\mathfrak{Rc}(X, Y) = g(\mathfrak{Rm}(\partial_i, X) \partial_i, Y),$$

Its components  $R_{jk} = \mathfrak{Rc}(\partial_j, \partial_k)$  are given in  $U \subset M$  by the contraction (see e.g., [56])

$$\begin{aligned} R_{jk} &= R_{ijk}^i, & \text{or, in terms of Christoffel symbols,} \\ R_{jk} &= \partial_i \Gamma_{jk}^i - \partial_k \Gamma_{ji}^i + \Gamma_{mi}^i \Gamma_{jk}^m - \Gamma_{mk}^i \Gamma_{ji}^m. \end{aligned}$$

Being a symmetric second-order tensor,  $\mathfrak{Rc}$  has  $\left(\frac{n+1}{2}\right)$  independent components on an  $n$ -manifold  $M$ . In particular, on a 3-manifold, it has 6 components, and on a 2D surface it has only the following 3 components:

$$R_{11} = g^{22} R_{2112}, \quad R_{12} = g^{12} R_{2121}, \quad R_{22} = g^{11} R_{1221},$$

which are all proportional to the corresponding coordinates of the metric tensor,

$$\frac{R_{11}}{g_{11}} = \frac{R_{12}}{g_{12}} = \frac{R_{22}}{g_{22}} = -\frac{R_{1212}}{\det(g)}. \quad (84)$$

Finally, the scalar curvature  $R$  is the trace of the Ricci tensor  $\mathfrak{Rc}$ , given in  $U \subset M$  by

$$R = g^{ij} R_{ij}.$$

For example, on a geometric sphere, we have the following relation between 3D Cartesian  $(y^i)$  and 2D polar coordinates  $(x^j)$ :

$$y^1 = R \cos x^1 \cos x^2, \quad y^2 = R \sin x^1 \cos x^2, \quad y^3 = R \sin x^2,$$

and the components of the metric tensor are

$$\{g_{ij}\} = \begin{Bmatrix} R^2 \cos^2 x^2 & 0 \\ 0 & R^2 \end{Bmatrix}, \quad \det(g_{ij}) = R^4 \cos^2 x^2,$$

so that we have only one component of the Riemann tensor,

$$R_{1212} = R^2 \sin^2 x^2.$$

Next, from (84) we get the components of  $\mathfrak{Rc}$

$$R_{11} = -\sin^2 x^2, \quad R_{12} = R_{21} = 0, \quad R_{22} = -\tan^2 x^2,$$

or

$$\{R_{ij}\} = \begin{Bmatrix} -\sin^2 x^2 & 0 \\ 0 & -\tan^2 x^2 \end{Bmatrix}.$$

Finally, for the scalar Ricci curvature,  $R = g^{ij} R_{ij}$ , we have

$$R = g^{11} R_{11} + g^{22} R_{22} = -\frac{2}{R^2} \tan^2 x^2.$$



Similarly, on a Riemannian  $n$ -manifold  $M$  of constant Gaussian curvature  $K$ , Ricci tensor is proportional to the metric tensor,

$$R_{ij} = -(n-1)Kg_{ij},$$

while Ricci curvature  $R$  is given by

$$R = -n(n-1)K.$$

## References

- [1] G. Nicolis, A. De Wit, Scholarpedia, **2**(9), 1475, (2007)
- [2] I. Prigogine, From Being to Becoming: Time and Complexity in the Physical Sciences. Freeman, San Francisco, (1980).
- [3] R. Friedrich, Group Theoretic Methods in the Theory of Pattern Formation, in Collective dynamics of nonlinear and disordered systems, Springer, Berlin, (2004).
- [4] M. Bode, Front-bifurcations in reaction-diffusion systems with inhomogeneous parameter distributions, Physica D 106 (1997) 270–286.
- [5] A.M. Turing, The Chemical Basis of Morphogenesis. Phil. Trans. Roy. Soc. London, B **237**, 37–72, (1952).
- [6] V. Ivancevic, T. Ivancevic, Geometrical Dynamics of Complex Systems. Springer, Dordrecht, (2006).
- [7] H.-G. Purwins, H.U. Bodeker, A.W. Liehr, Dissipative Solitons in Reaction-Diffusion Systems, in Dissipative Solitons (ed. N. Akhmediev, A. Ankiewicz), Lecture Notes in Physics, Springer, (2005).
- [8] S.V. Gurevich, S. Amiranashvili, H.-G. Purwins, Breathing dissipative solitons in three-component reaction-diffusion system. Phys. Rev. E**74**, 066201, (2006).
- [9] T. Roose, S.J. Chapman, P.K. Maini, Mathematical Models of Avascular Tumor Growth. SIAM Rev. **49**(2), 179–208, (2007).
- [10] Gierer, A., H. Meinhardt, A theory of biological pattern formation. Kybern. **12**, 30-39, (1972).
- [11] H. Meinhardt, Scholarpedia, **1**(12), 1418, (2006).
- [12] Field, R.J., Kőrös, E., Noyes, R.M., Oscillations in chemical systems. J. Amer. Chem. Soc. **94**, 8649–8664, (1972).

- [13] Tyson, J.J., A quantitative account of oscillations, bistability and travelling waves in the Belousov-Zhabotinskii reaction, in *Oscillation and Travelling Waves in Chemical Systems*, eds. Field, R. J., Burger, M., Wiley-Intersc., New York, (1985).
- [14] Nielsen, K., Hynne, F., So rensen, P.G., Hopf bifurcation in chemical kinetics, *J. Chem. Phys.* textbf94, 1020–1029, (1991).
- [15] Field, R.J., Oregonator, Scholarpedia, textbf2(5), 1386, (2007).
- [16] M.I. Rabinovich, A.B. Ezersky, P.D. Weidman, *The Dynamics of Patterns*, World Scientific, Singapore, 2000.
- [17] FitzHugh R., Impulses and physiological states in theoretical models of nerve membrane. *Biophys. J.* **1**, 445-466, (1961).
- [18] Nagumo J., Arimoto S., Yoshizawa S., An active pulse transmission line simulating nerve axon. *Proc IRE.* 50, 20612070, (1962).
- [19] T. Ivancevic, L. Jain, J. Pattison, A. Hariz, *Nonlinear Dynamics and Chaos Methods in Neurodynamics and Complex Data Analysis. Nonl. Dyn.* (Springer) (to appear)
- [20] Schöner, G., *Dynamical Systems Approaches to Cognition*. In: *Cambridge Handbook of Computational Cognitive Modeling*. Cambridge University Press. R. Sun (ed), (2007)
- [21] Amari, S., Dynamics of pattern formation in lateral-inhibition type neural fields. *Biol. Cybern.* **27**, 77–87, (1977)
- [22] Grote, C., Schöner, G., Context-sensitive generation of goal-directed behavioral sequences based on neural attractor dynamics. *Proceedings of the ISR/ROBOTIK2006 Joint Conference on Robotics*, Munich, Germany, May, (2006)
- [23] V. Ivancevic, T. Ivancevic, *High-Dimensional Chaotic and Attractor Systems*. Springer, Berlin, (2006).
- [24] Ivancevic, V., Ivancevic, T.: *Natural Biodynamics*. World Scientific, Singapore, (2006)
- [25] Ivancevic, V., Ivancevic, T., *Neuro-Fuzzy Associative Machinery for Comprehensive Brain and Cognition Modelling*. Springer, Berlin, (2007)
- [26] Ivancevic, V., Ivancevic, T., *Computational Mind: A Complex Dynamics Perspective*. Springer, Berlin, (2007)

- [27] D. Mackenzie, Perelman Declines Math's Top Prize; Three Others Honored in Madrid, *Science* **313**, 1027, (2006).
- [28] S.T. Yau, Structure of Three-Manifolds - Poincaré and geometrization conjectures. talk given at the Morningside Center of Mathematics on June 20, (2006).
- [29] V. Ivancevic, T. Ivancevic, *Complex Dynamics: Advanced System Dynamics in Complex Variables*. Springer, Dordrecht, (2007)
- [30] Ivancevic, V., Ivancevic, T.: *Applied Differential Geometry: A Modern Introduction*. World Scientific, Singapore, (2007)
- [31] V. Ivancevic, Symplectic Rotational Geometry in Human Biomechanics, *SIAM Rev.* **46**(3), 455–474, (2004)
- [32] S. Hawking, R. Penrose, *The Nature of Space and Time*, Princeton Univ. Press, 1996.
- [33] R. Penrose, Singularities and Time-Asymmetry, in *General Relativity: An Einstein Centenary Survey*, (ed. S. Hawking, W. Israel), 581-638, Cambridge Univ. Press, (1979).
- [34] G. Perelman, The entropy formula for the Ricci flow and its geometric applications, arXiv:math.DG/0211159
- [35] G. Perelman, Ricci flow with surgery on three-manifolds, arXiv:math.DG/0303109
- [36] R.S. Hamilton, Three-manifolds with positive Ricci curvature, *J. Diff. Geom.* **17**, 255-306, (1982)
- [37] J. Milnor, Towards the Poincaré Conjecture and the Classification of 3-Manifolds, *Not. Am. Math. Soc.* **50**(10), 1226-1233, (2003)
- [38] M.T. Anderson, Geometrization of 3-manifolds via the Ricci flow, *Not. Am. Math. Soc.* **51**(2), 184-193, (2004)
- [39] R.S. Hamilton, Four-manifolds with positive curvature operator, *J. Dif. Geom.* **24** (1986) 153-179.
- [40] R.S. Hamilton, The Harnack estimate for the Ricci flow, *J. Dif. Geom.* **37** (1993) 225-243.
- [41] R.S. Hamilton, The Ricci flow on surfaces, *Cont. Math.* **71** (1988), 237-261.
- [42] R.S. Hamilton, Non-singular solutions of the Ricci flow on three-manifolds, *Comm. Anal. Geom.*, **7**(4), 695-729, 1999.

- [43] W. Thurston, Three-dimensional manifolds, Kleinian groups and hyperbolic geometry, *Bull. Amer. Math. Soc.* **6** (1982) 357-381.
- [44] H.D., Cao, B. Chow, Recent developments on the Ricci flow, *Bull. Amer. Math. Soc.* **36** 59-74, 1999.
- [45] Chow, B., Knopf, D. The Ricci flow: An introduction, *Mathematical Surveys and Monographs*, AMS, Providence, RI, 2004.
- [46] S.Y. Hsu, Some results for the Perelman LYH-type inequality, *arXiv:math.DG/0801.3506*
- [47] P. Li, S.T. Yau, On the parabolic kernel of the Schrödinger operator. *Acta Math.* **156**, 1986, 153–201.
- [48] R. Ye, The log entropy functional along the Ricci flow. *arXiv:math.DG/0708.2008v3*
- [49] J. Li, First variation of the Log Entropy functional along the Ricci flow, *arXiv:math.DG/0712.0832*
- [50] M.J. Ablowitz, D.J. Kaup, A.C. Newell, H. Segur, Method for solving the sine-Gordon equation. *Phys. Rev. Let.* **30**, 1262–1264, (1973).
- [51] N.N. Akhmediev, V.M. Eleonskii, N.E. Kulagin, First-order exact solutions of the nonlinear Schrödinger equation. *Th. Math. Physics* **72**, 809–818, (1987).
- [52] Wikipedia, the free encyclopedia, 2008.
- [53] Kohler G, Milstein C., Continuous cultures of fused cells secreting antibody of pre-defined specificity. *Nature*, 256, 495, (1975).
- [54] Francis RJ, Sharma SK, Springer C, et al. A phase I trial of antibody directed enzyme prodrug therapy (ADEPT) in patients with advanced colorectal carcinoma or other CEA producing tumours. *Br J Cancer* 2002; 87: 600-607.
- [55] Carter P, Improving the efficacy of antibody-based cancer therapies. *Nat. Rev. Cancer*, 1, 118-129, (2001).
- [56] C. Misner, K. Thorne, J.A. Wheeler, *Gravitation*, W.H. Freeman and Company, (1973).
- [57] Kosko, B., *Neural Networks and Fuzzy Systems, A Dynamical Systems Approach to Machine Intelligence*. Prentice–Hall, New York, (1992)
- [58] Haykin, S., *Adaptive Filter Theory*. Prentice–Hall, Englewood Cliffs, (1991)

- [59] Hopfield, J.J., Neural networks and physical systems with emergent collective computational abilities. *Proc. Natl. Acad. Sci. USA* **79**, 2554, (1982)
- [60] Hopfield, J.J., Neurons with graded response have collective computational properties like those of two-state neurons. *Proc. Natl. Acad. Sci. USA*, **81**, 3088–3092, (1984)
- [61] Hebb, D.O., *The Organization of Behavior*, Wiley, New York, (1949)
- [62] Hoppensteadt, F.C., Izhikevich, E.M., *Weakly Connected Neural Networks*. Springer, New York, (1997)
- [63] Haken, H., *Synergetics: An Introduction* (3rd ed). Springer, Berlin, (1983)
- [64] Ivancevic, V., Ivancevic, T.: *Natural Biodynamics*. World Scientific, Singapore, (2006)
- [65] V. Volterra, Variations and fluctuations of the number of individuals in animal species living together, in *Animal Ecology*. McGraw-Hill, (1931).